COOPERATIVE RESEARCH CENTRE FOR **CATCHMENT HYDROLOGY**

REGIONAL MODELS OF STREAM CHANNEL METRICS

TECHNICAL REPORT
Report **05/16**
June 2005

Michael Stewardson / Ron DeRose / Ciaran Harman

COOPERATIVE RESEARCH CENTRE FOR
CATCHMENT HYDROLOGY

Stewardson, Michael.

Regional Models of Stream Channel Metrics

Bibliography

ISBN 1 920813 34 9.

1. Stream measurements - Australia. 2. Streamflow - Australia. I. DeRose, Ronald Charles. II. Harman, Ciaran. III. Cooperative Research Centre for Catchment Hydrology. IV. Title.
(Series: Report (Cooperative Research Centre for Catchment Hydrology); 05/16).

551.4830994

Keywords

Channels
Rivers
Geometry
Geomorphology
Models
Hydraulics
Catchment hydrology
Regression analysis
Surveys
Equations
Flow rates
Uncertainty

Regional Models of Stream Channel Metrics

Michael Stewardson, Ron DeRose and Ciaran Harman

Technical Report 05/16

June 2005

Preface

There is increasing concern for the remote impacts of land and water resources management decisions. The CRC for Catchment Hydrology has devoted considerable attention to developing models for assessing these impacts. This report provides models of channel geometry for use in these catchment-scale models. Channel geometry is a primary factor controlling the flux of water and sediment through catchments as well as hydrologic interactions between the channel and floodplain surface and subsurface flow pathways. This report describes the development of empirical equations to estimate hydraulic geometry metrics throughout river networks based on a large set of river surveys in Victoria, Australia. Channel metrics include bankfull width, depth, shape, slope and discharge and at-a-station hydraulic geometry parameters. All models are provided with some indication of their error so users can assess the uncertainty in their model predictions. In some cases, channel metric models do not perform so well, although measurement and sample errors can also be very large if practitioners choose to survey rather than model channel hydraulics. An estimate of sample and measurement errors for some metrics is provided in report. Data sets used in this study are available via the internet at www.toolkit.net.au.

Mike Stewardson,
Program Leader - River Restoration
CRC for Catchment Hydrology

Acknowledgements

Channel survey data were initially collated by Susan Hayes. We are very grateful to EarthTech, Sinclair Knight Merz and the Department of Sustainability and Environment for freely providing channel survey data. Numerous people provided advice on this project and we particularly would like to thank Brian Finlayson and Ian Rutherfurd from SAGES at The University of Melbourne, Dean Judd (Monash University) for his suggestion to consider meander wavelength as an independent variable. We gratefully acknowledge Tristram Miller formerly of CSIRO for the tedious task of collating, processing and georeferencing hydrological records and Yun Chen and Arthur Read of CSIRO Land and Water for their expert GIS knowledge in the development of automating measurement of channel sinuosity and meander wavelength.

Executive Sumary

The geometry of rivers affects many of the issues of concern in catchment management, including transmission of flow, sediment and nutrients, environmental flows, physical habitat conditions and flooding. This report describes the methods and results of a core project in the Cooperative Research Centre for Catchment Empirical model are developed to relate channel metrics including dimensions, bankfull discharge, channel slope and at-a-station hydraulic geometry to catchment data generally available in the populated regions of Australia. Models should be tested for their applicabability in other regions. However, the study sites represent a broad range of climates, flow regimes, channel sizes and management impacts from across Victoria and are generally applicable, at least in this region. The models will be useful in catchment modelling applications where changes in channel form over time are not important. To establish appropriate confidence in model performance, we provide error terms. Anyone using these models can perturb the error terms to evaluate sensitivity of their results to model uncertainties.

List of Figures

List of Tables

1. Introduction

The geometry of rivers affects many of the issues of concern in catchment management, including transmission of flow, sediment and nutrients. Channel geometry is an important consideration in the design of environmental flow regimes in regulated rivers and is one of the primary factors determining physical habitats in channels and surrounding floodplains. Changes to the river form and the associated processes of riverbank erosion are one of the potential consequences of altered flow regimes, future land use change and future climate change. This report describes the methods and results of a core project in the Cooperative Research Centre for Catchment Hydrology to model links between catchments and channel geometry for use in the Catchment Modelling Toolkit.

In this study we develop empirical models to predict channel dimensions from catchment data generally available in the populated regions of Australia. This report describes the analysis of (i) 93 channel surveys for calculating channel metrics and (ii) catchment data likely to predict variations in channel form. Empirical models are established using regression analysis to relate these two data sets. There are some conceptual models of the geomorphic controls on river channels which we use to select appropriate independent variables for these regression analyses. However, because the approach is empirical, models should be tested for their applicabability in other regions. However, the study sites represent a broad range of climates, flow regimes, channel sizes and management impacts from across Victoria and are generally applicable, at least in this region.

Despite over 100 years of research, beginning in the 19th Century with the development of regime equations for stable canal design, the theoretical basis for quantitative modelling of channel form is weak. Hypotheses have been proposed to explain the effect of geomorphic controls including valley slope, boundary material and regimes of sediment and flow, but in most cases, testing is limited to flume experiments or ideal field conditions. Theoretical approaches could be tested using our data set, but these models are unlikely to perform well in natural channels without considerable calibration, which limits their generality. There is a strong need for improvements in this theoretical basis. Indeed the data sets and our results may assist with this research but it is not a focus of this study.

It would be convenient if we could assume that the data base of channel surveys used in this study only included rivers in dynamic equilibrium with their geomorphic controls. However, channels in Australia, particularly in lowland areas, have been modified by flow regulation, channel incision, deposition of sand slugs, channel widening, direct engineering modifications for flood and erosion control and other catchment disturbances. In reality, our data set includes river channels that have been modified since European settlement and may still be adjusting to historic catchment and riparian disturbances. Natural events such as bushfire and extreme floods can also modify channel form with effects persisting for some years after the event. In some cases, rivers may naturally display episodic change with subsequent recover such as channel avulsion. These channel changes complicate development of channel metrics models and may appear in our models as an error term. A parallel research effort in the CRC for Catchment Hydrology is examining models of channel adjustment to modifications in the geomorphic controls over time and will be reported separately. This research should help to improve our capacity to predict channel changes.

The empirical models developed in this study will be useful in catchment modelling applications where changes in channel form over time are not important. For example, modelling effects of flow regulation on physical habitats in the absence of geomorphic changes, or flood and sediment routing in stable channels. It is unrealistic to expect this broad-scale empirical study to provide highly accurate models. In some cases, errors may be too large for models to be useful in applications. To establish appropriate confidence in model performance, we provide error terms. Anyone using these models can perturb the models, based on these error terms to evaluate sensitivity of their results to model uncertainties.

Chapter 2 describes the earlier methods used to model channel metrics, in particular hydraulic geometry and regime equations. To develop our models, we have collated a large set of channel surveys from Victorian rivers. A one-dimensional hydraulic model is constructed for each of 93 channel surveys across Victoria. These data and the hydraulic modelling are described in Chapter 3. Chapter 4 describes how we use GIS data, streamflow gauging and other extensive data sets to calculate catchment and riparian attributes which are likely to predict channel metrics. We mainly use data that is commonly available in Australia to ensure models are generally applicable. The empirical models are developed in Chapter 5 while Chapter 6 provides a discussion of the results.

2. Methods for Modelling Channel Metrics

2.1 Regime Equations for Stable Canals

A stream is said to be in regime if its channel has achieved a stable (i.e., equilibrium) form as a result of its flow and sediment characteristics. Inherent in this concept is the notion that given time, a channel will reach an equilibrium form by self-adjustment of the channel boundary, assuming that imposed conditions do not change in the long-term (Blench 1951; Graf 1971). Regime equations have been developed to relate bankfull channel geometry to the environmental variables which determine channel form. These equations are mostly empirical.

Much of the early work on regime channels was based on observations of stable canals (e.g. Kennedy 1895, Lindley 1919, Lacey 1929). Later developments of these regime equations showed that the relationship between channel width, depth slope and discharge is dependant on the material composition of bed and banks and on the sediment load being transported by the river (Blench 1951, Blench 1957, Graf 1971). Simons *et al.,* (1962) gives the most general form for these equations as:

$$\overline{W} = 1.63K_1\sqrt{Q},$$

$$D = 1.33K_2Q^{0.36} \quad (R \le 2.1\ m)\ or$$

$$D = 0.61 + 1.08K_2Q^{0.36}\ (R \ge 2.1\ m),\ \text{and}$$

Where W is top width, D is channel depth, R is hydraulic radius and Q is the capacity of the channel (all converted from source to S.I. units). Henderson (1966) provided estimates for the coefficients (Table 2).

2.2 Downstream Hydraulic Geometry Relations

Leopold *et al.,* (1964) introduced downstream hydraulic geometry to describe regime relations between width (W), mean depth (D) and mean velocity (U) for the bankfull channel and some meaningful discharge (Q) such as the mean flow, bankfull flow or flood magnitude of an agreed recurrence interval of exceedance. These relations commonly take the form

$$W = aQ^b \tag{1}$$

$$D = cQ^f \tag{2}$$

$$U = kQ^m \tag{3}$$

The six parameters (a, b, c, f, k and m) are normally estimated by regression using survey data. To maintain continuity the sum of the exponents ($b+f+m$) and the product of the constants ($a.c.k$) must equal one if bankfull discharge is used for the downstream hydraulic geometry relations. Various studies have derived empirical downstream hydraulic geometry equations using either the mean discharge ($\bar{Q}$) or bankfull discharge (Q_{bf}) for particular rivers or regions.

The downstream hydraulic geometry parameters could be affected by sediment supply, downstream fining of bank sediments, plan form geometry, bank vegetation

Table 1. Henderson s (1966) for regime coefficients (Eqns. 17).

Types of channel	K_1	K_2
Sand bed and banks	3.5	0.52
Sand bed, cohesive banks	2.6	0.44
Cohesive bed and banks	2.2	0.37
Coarse non cohesive material	1.75	0.23
Sand bed, cohesive banks, heavy sediment load	1.70	0.34

and processes of bank erosion can force longitudinal changes in channel properties without much change in discharge (Schumm 1960, Schumm 1977, Andrews 1984, Brierly and Hickin 1985, Hey and Thorne 1986, Huang and Nanson 1997, Pitlick and Cress 2002).

2.3 Theoretical Regime Equations

The empirical regime equations expressed as downstream hydraulic geometry equations may provide some indication of how channels will respond to catchment changes, but their weak theoretical basis means they do not provide strong insight into the fundamental controls on channel geometry (Eaton and Millar 2004). Theoretical regime equations have been developed by solving equations for continuity, flow resistance and sediment transport. However an additional equation is required to solve these equations for equilibrium conditions. A number of equations have been suggested, usually relying on the argument that the channel adjusts until some hydraulic parameter is maximised or minimised (hence termed extremal hypotheses).

Some of these hypotheses have been shown to produce hydraulic geometry relations more or less consistent with those derived empirically. However, these hypotheses have been criticised because the theoretical basis is not clear (ASCE 1998). Also, the equations require the assumption of conditions that are unlikely in natural channels. They generally require assumptions of a straight channel with uniform flow conditions. However channel slope is one of the variables that adjusts to establish the so called regime state and presumably these adjustments are through changes in sinuosity. Flow resistance is assumed to be the result of grain roughness alone, which is unlikely except in straight gravel bed streams with no instream vegetation. A uniform sediment flux is also required. However, channel adjustments to achieve the equilibrium state require deposition and erosion which continuously alters sediment flux along a river and results in meander migration.

2.4 At-a-Station Hydraulic Geometry

Leopold and Maddock (1953) introduced at-a-station hydraulic geometry relations which take the same form as those for downstream hydraulic geometry except that they describe variation in width, mean depth and mean velocity (U) at a cross-section with discharge (Q) rather than variations between sites. As with the downstream hydraulic geometry, continuity requires that the sum of exponents and the product of coefficients is 1. It might be expected that variation in the at-a-station hydraulic geometry parameters is, in part, the result of variations in channel characteristics. However, the location of the cross-sections within a reach (e.g. whether in a pool or riffle) will also affect the at-a-station hydraulic geometry (Knighton 1975; Singh and McConkey 1989). The range of discharges (Lewis *et al.,* 1996) the method used (Rhoads 1992) and error in hydraulic data (Leopold *et al.,* 1964) when calculating hydraulic geometry parameters can also affect results.

At-a-station hydraulic geometry refers specifically to hydraulic variations with discharge at a single cross-section (Leopold *et al.,* 1964; Knighton 1984). Recently, there have been efforts to develop hydraulic geometry relations for the distribution of hydraulic parameters within a reach based on surveys of multiple cross-sections. This approach can be described as Reach Hydraulic Geometry (Stewardson 2005). Some studies have examined reach hydraulic geometry for studies of fluvial processes (Western *et al.,* 1997; Buhman *et al.,* 2002) or to assist stream habitat assessment (Singh and McConkey 1989; Jowett 1998; Lamouroux and Suchon 2002; Lamouroux and Capra 2002). In all these studies, the arithmetic mean has been used and consequently the exponents (b, f and m) do not necessarily sum to one (Singh and McConkey 1989, Stewardson 2005).

2.5 Channel Shape

Channel shape has a controlling influence on at-a-station hydraulics. However, few studies have examined factors controlling channel shape compared with bankfull dimensions. In a natural channel, shape includes not only the average dimensions but also the

longitudinal variation in these dimensions introduced by bars, benches and variations in bank profiles and channel width.

The simplest characteristic of channel shape is the width to depth ratio at bankfull. Form ratio (ie width/depth at bankfull) is considered a function of the channel perimeter sedimentology (Richards, 1982). Schumm (1960) found a relationship between percent silt and clay in the channel boundary sediments (M) and the width to maximum depth ratio (W/D_m):

$$W / D_m = 255M^{-1.08}$$

Schumm (1960) suggested that aggrading and degrading streams generally had respectively higher and lower width to depth ratios than predicted by this equation. However, establishing reliable general relationships based on empirical studies is difficult because large rivers are almost always wide, deep, gently sloping with fine bed material. Interpreting correlation in these parameters is difficult because of this covariance.

3. Hydraulic Data

3.1 Cross-Section Surveys

The channel survey data used in this study consists of cross section surveys obtained from agencies, consultants and researchers. The initial intent for the survey database is for the channel metrics modelling described in this report, but it is stored and documented in a systematic way to facilitate use in future projects. Four criteria had to be satisfied for data to be included in the database:

(1) surveys extended up to bank-full stage

(2) elevations were all surveyed to the same datum (not necessarily AHD)

(2) the location of the surveys is known within 500 m, and

(3) there are at least three cross-sections for the survey.

The final data set included 117 surveys. These were supplied from Earth Tech, the Victorian Department of Sustainability and Environment Floodplains Unit, Sinclair Knight Mertz, the Victroian Environmental Protection Agency and internal data bases of researchers involved in the project (Michael Steardson and Tony Ladson). Of these 19 are floodplain surveys that are yet to be digitised, and not of insufficient quality to warrant the effort. Another 9 reaches were very long, and were consequently split into between 2 and 4 sections less than 10 km long. Thus the total number of useable reaches in the database is 114. Reach locations are shown in Figure 1 and reach length and cross-section number is shown in Figure 2. There are 1,213 cross-sections within the collated data base.

Of the 114 reaches, 11 were discarded because they were located along secondary channels in anastamosing rivers and a further 10 were discarded because hydraulic models errors were assessed to be particularly large at these sites. These second group of sites were identified as those where model errors (refer to Chapter 4) in bankfull width, depth or discharge were greater than 20% (calculated as standard deviation of replicate estimates divided by the best estimate). This left 93 surveys for use in this study.

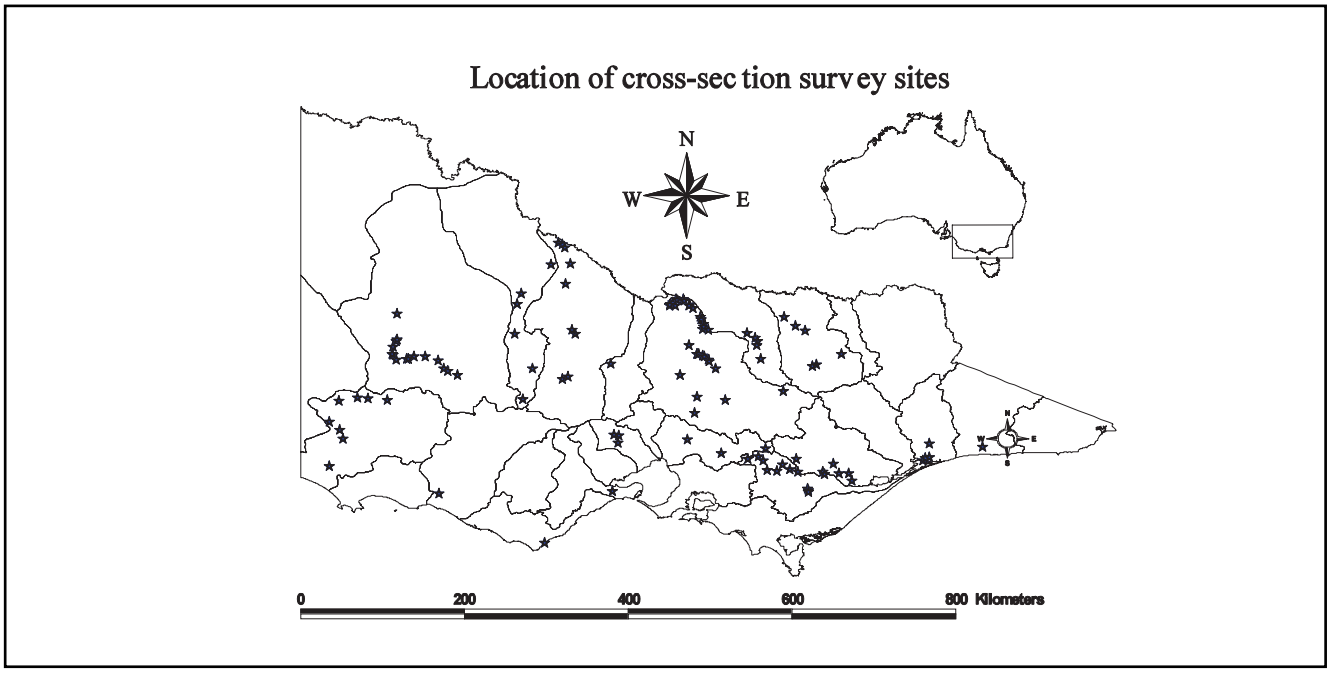

Figure 1. Location of Channel Surveys.

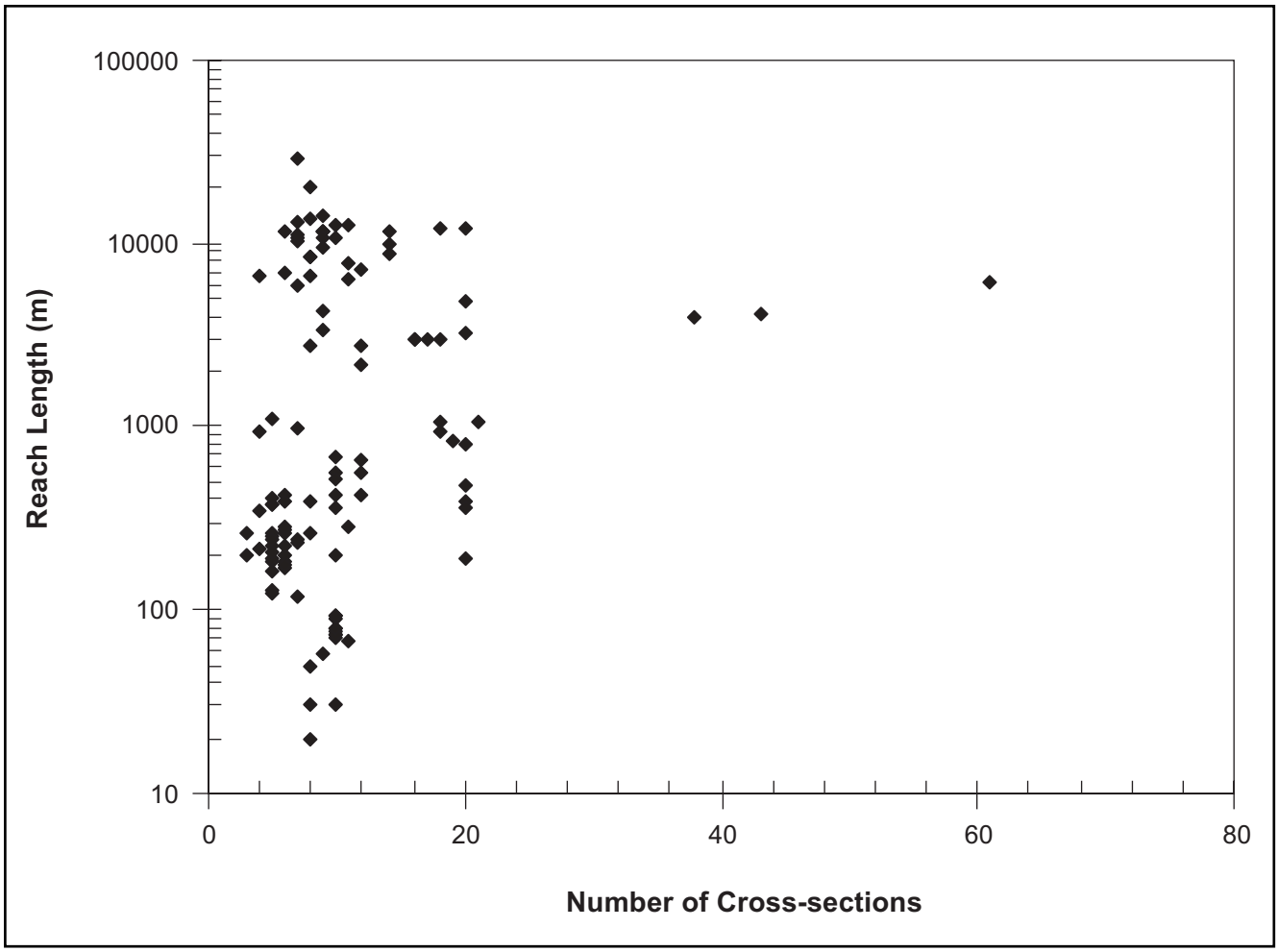

Figure 2. Reach Length and Number of Cross-sections for each of the 114 Surveys Collated for this Study.

3.2 Hydraulic Modelling

A one-dimensional hydraulic model was used to model water surface profiles for the full range of flows up to bankfull level. This model was based on the same basic equations as HEC-RAS (Brunner 2001), but was implemented in MATLAB™ to allow model runs to be batched and their outputs collated automatically[1]. The model was validated against HEC-RAS outputs. The two principle pieces of information required for one dimensional modelling of natural channels (apart from channel geometry) are the roughness at each cross section and the downstream boundary condition. Manning's n can vary with discharge, particularly at low flows.

Lang *et al.,* (2004) reviewed the performance of 15 empirical equations in 4 Australian streams for estimating channel roughness. They concluded that the Dingman and Sharma (1997) and Riggs (1976) models performed the best. We chose to use the Dingman-Sharma equation which gives Manning's n as:

$$n=0.217A^{1.173}R^{0.267}S^{0.156}$$

Where n is Manning's n, A is cross sectional flow area, R is hydraulic radius and S is energy slope. Since this model only relies on channel geometry, estimates of Manning's n can be obtained even if no other information apart from the channel survey data is available. The Dingman-Sharma equation is only applicable for flows greater than 1 m^3/s so this is the lower limit on the range of flows modeled for each channel.

This empirical approach was preferred to estimates of Manning's n calibrated using surveyed water surface profiles for two reasons. Firstly, there was a limited amount of data available at the sites for calibration. Secondly, the errors in the Dingman and Sharma (1997) model are fully specified, allowing a detailed uncertainty analysis to be carried out on the final result.

The one-dimensional model requires that the water level at the downstream cross-section is known (sometimes referred to as the downstream boundary condition). The downstream boundary can have a strong influence on the calculated water surface levels for reaches that are short or have few hydraulic controls. The downstream boundary condition of a one dimensional hydraulic model can be specified in a number of ways. The most accurate method is to use a known rating curve, but in the absence of this, a water surface slope is often assumed and used to calculate the normal depth of flow using Manning's equation. In this study we estimated slope at the downstream cross-section from 1:25,000 topographic maps with 10 m height contour for steeper rivers and surveyed flood profiles for low gradient rivers.

3.3 Method for Identifying Bankfull Levels

The Dictionary of Geography defines bank-full stage as "The state of flow in a river when, because of the high volume of water, no river banks are exposed. This stage is reached just prior to the flooding stage when the brim-full river outflows its banks". However, identifying the actual stage at which this flow occurs is problematic. Identifying bankfull stage is complicated by highly variable of bank morphology and the difficulty of deciding where the top of the river banks occurs and floodplains begins.

Most methods for identifying bankfull stage require direct field observations (Leopold *et al.,* 1964) including identification of the principal sedimentary surface and boundary features such as vegetation. However these field observations were not possible for any of the surveys collated in this project. In our project we used the following procedure:

- Bankfull level was first assessed visually at each cross section by looking for the break in the slope of the bank.

[1] The one-dimensional model also represented form drag using conventional approaches based on rates of expansion and contraction along the reach. An eddy loss equal to 0.3 times the change in velocity head was included where the width of cross-sections expanded by greater than 10%. Similarly a 0.1 eddy loss was used for cross sections contracting by 10%. See Henderson (1966) for a description of this procedure.

- The bankfull level was set at the lower of the bank points on either side of the channel.
- The bankfull flow was identified as the flow with a water surface profile closest to the bankfull levels identified for cross-sections along the reach. More specifically, the bankfull flow was determined to be the flow Q that minimised the value of:

$$\sum_{i=1}^{n}(Z_i(Q)-Z_{Bi})^2$$

Where n is the number of cross sections, Z_i is the water surface level and Z_{Bi} is the bankfull level estimated visually at cross section i.

For the data set in this study, the problem of identifying bankfull level was compounded where the channel survey did not extend across the floodplain. These sites presented two problems. Firstly, we had to rely on advice of data providers that the survey was indeed to the top of bank. Secondly, when flow exceeded the top survey point on either side of the channel, the hydraulic model was forced to assume that no water spilled onto the floodplain, creating errors in the model near bankfull.

For this reason a quality index was assigned to each cross section, according to how confident we could be that the assigned bankfull level was indeed the top of bank. These four ratings (in order of increasing confidence) were:

1. No indication of top of bank, survey end-points are assumed to be top of bank.
2. Partial information of top of bank or flood plain on one or both sides of cross section. Position of channel with regards to floodplain unclear.
3. Partial information of top of bank or flood plain on one or both sides of cross section. Position of channel with regards to floodplain clear.
4. Extensive over-bank survey. Position of channel with regards to flood plain clear.

These ratings could then be averaged for a reach to give an overall confidence in the bankfull level.

3.4 Calculating Channel Metrics

In this study we develop empirical models for 18 channel metrics (Table 2). Channel metrics were calculated from the output of the 1-D hydraulic modeling described above. A MATLAB script was created to automate this procedure. At each cross-section the modelled water surface level was compared with the cross-section survey points to obtain the wetted polygon of the stream cross-section. Linear interpolation was used between survey points. This polygon was used to calculate the stream's cross-section area, top-width, mean depth, maximum depth, velocity, wetted perimeter and Froude number.

These cross-section metrics were combined into reach metrics using the mean and standard deviation. A $\log_e$ transformation of the cross-section metrics is used to calculate the reach metrics. For example mean width is calculated as:

$$\overline{W} = \exp\left(\mu(\ln W_{1\ldots m})\right) = \exp\left(\sum_{i=1}^{m}\frac{\ln(W_i)}{m}\right)$$

and standard deviation of width is calculated as

$$\sigma(\ln W) = \sqrt{\frac{\sum_{i=1}^{m}\left(\ln W_i - \overline{\ln W}\right)^2}{m}} = \sqrt{\frac{\sum_{i=1}^{m}\left(\ln\frac{W_i}{\overline{W}}\right)^2}{m}}$$

Where m is the number of cross-sections and W_i is the width of the i^{th} cross-section. The $\log_e$ transformation is used so that the product of reach-mean velocity, depth and width equals discharge. This would not hold true if the arithmetic mean was used.

The original at-a-station hydraulic geometry equations use a single linear function. However, Bates (1990) recognised the existence of a breakpoint in these relations and suggests using two linear functions to better represent variations with discharge. We used Bates (1990) log-piecewise linear model of at-a-station hydraulic geometry to fit a hydraulic geometry relationship between the reach hydraulic metrics and Q. For details of the Bates (1990) method the reader is referred to the original paper. The method uses a piecewise linear model for the log-transformed Q and channel metric.

Table 2. Mean and Variance in Channel Metrics and Estimated Proportion of this Variance Introduced by Sample and Model Errors (S.I. units are used for all metrics).

Metric Name	Symbol	Transform[1]	Mean Value[2]	Variance[2]	Uncertainty[3]
bankfull discharge	Q_{bf}	ln	4.52	1.357	0.04
bankfull energy slope	s_{bf}	ln	-6.86	1.616	0.34
bankfull reach-mean width	W_{bf}	ln	3.47	0.655	0.03
bankfull reach-mean depth	D_{bf}	ln	0.908	0.577	0.07
ratio of bankfull width and depth	W_{bf}/D_{bf}	ln	2.56	0.387	-
ratio of bankfull wetted perimeter and width	P_{bf}/W_{bf}	ln	0.0737	0.0349	-
ratio of bankfull maximum depth and mean depth	Dm_{bf}/D_{bf}	ln	0.464	0.120	-
variation in bankfull width	σ_{Wbf}	-	0.243	0.124	0.42
variation in bankfull depth	σ_{Dbf}	-	0.203	0.123	0.47
change point discharge for at-a-station hydraulic geometry	Q_{CP}	ln	2.13	0.863	0.40
at-a-station hydraulic geometry parameters	θ_{W1}	-	2.82	0.34	0.08
	θ_{W2}	-	0.235	0.0792	0.40
	$\theta_{W\frac{3}{4}}$	-	0.0112	0.0661	0.71
	a_2	ln	2.36	0.669	-
	θ_{D1}	-	-0.201	0.287	0.43
	θ_{D2}	-	0.414	0.082	0.66
	$\theta_{D\frac{3}{4}}$	-	0.034	0.0642	0.75
	c_2	ln	-1.08	0.468	-

1 Transformations were applied were necessary to normalise sample distributions of variables.
2 Mean and variance is provided for the transformed values where transformations are specified.
3 Uncertainty is the proportion of variance in estimated metric values associated with model and sample errors.
4 a_2 and c_2 are the coefficients for width and depth at-a-station hydraulic geometry relations for flows exceeding the change point discharge.

Since it involves two linear functions, Bates log-piecewise regression model yields four parameters for the hydraulic geometry relationship: α_{P1} and α_{P2} are the intercepts and β_{P1} and β_{P2} are the coefficients of the two linear fitted functions (log-log transformed variables) relating a channel metric P to discharge. The change-point for the two-part relation is defined by the intercept of the two linear equations. Following Bates suggestion we report these in a slightly modified form using the following parameters:

the value of the parameter at the change point (log transformed)

$$\theta_{P1} = \alpha_{P1} + \beta_{P1}\gamma_{P1}$$

the average coefficients (exponents in the linear domain)

$$\theta_{P2} = (\beta_{P1} + \beta_{P2}) / 2$$

the difference in the coefficients between the upper and lower parts of the relation

$$\theta_{P3} = (\beta_{P2} - \beta_{P1}) / 2$$

the discharge corresponding to the change point (log transformed)

$$\gamma_P = (\alpha_{P1} - \alpha_{P2}) / (\beta_{P2} - \beta_{P1})$$

If the upper and lower regimes are identical (ie there is no real breakpoint) the value of θ_{P3} approaches zero. Furthermore, if the break point occurs at the same flow for width, depth and velocity (that is $\gamma_W = \gamma_D = \gamma_U = \gamma$) then the exponents for both the upper and low hydraulic geometry relations will still sum to unity.

3.5 Uncertainty in Channel Metrics

The channel metrics are subject to uncertainty associated with possible errors in the hydraulic modelling and sampling cross-section to represent the conditions along an entire reach. We have quantified these uncertainties using a combination of Monte Carlo and bootstrap sampling. The bootstrap procedure is used to represent uncertainty associated with sampling. The Monte-Carlo analysis is used to represent the combined effects of sample errors and model errors associated with estimation of Manning n and the downstream water surface slope in the hydraulic model. The detail of this analysis are provided in Appendix I.

The primary result of the analysis is an estimate of the variance in each hydraulic metric introduced by sample and model errors. We cannot expect our regional models to explain this variance. Hence, the proportion of the variance in channel metrics explained by the regional models (expressed as the correlation coefficient, r^2, for the multivariate regression equations) is effectively capped at less than 100%. Larger model and sample errors reduce the portion of variance one could expect to explain with the regional models. Variance introduced for each channel metric as a consequence of model error was estimated using the Monte Carlo and bootstrap procedure. The results are presented in Table 2.

4. Catchment and Riparian Data

The models of channel dimensions are intended for application through populated areas of Australia. For this reason, it must be possible to derive independent variables (i.e. model input) using commonly available data. We calculated 27 such parameters (Table 3) which may be correlated with channel metrics. These were derived for each of the 93 channel survey sites. Indeed, in most cases, they were derived for rivers throughout Victoria using automated GIS procedures. Natural Log_e transformations were required in most cases to normalise the parameters (Table 3).

Table 3. Parameters Derived from Regional Data Sets Considered as Independent Variables for Correlation with Channel Metrics.

Symbol	Variable	Units	Data Source	Transform*
C_AREA	catchment area	km^2	9” national digital elevation model (DEM)	Ln
DEM_S	channel gradient		DEM elevations corrected for sinuosity	Ln
SLOPE	bankfull energy slope	-	Slope from one-dimensional hydraulic model	Ln
MEAND	meander wavelength	m	VicHydro GIS coverage of Victorian streams	Ln
SIN	channel sinuosity	-	VicHydro GIS coverage of Victorian streams	-
VBF_MAX	valley bottom flatness	-	9” DEM	-
USPWC	percent woody cover in the upstream catchment	%	Bureau of Rural Sciences Data	-
RIP_COV	riparian canopy cover	-	BRS 25 m woody cover buffered to 40 m either side of channel	-
CATCH_S	catchment slope = (mean catchment elevation - site elevation) / L_MAX_US	-	9” DEM	Ln
CATCH_SH	catchment shape = C_AREA / L_MAX_US2	-	9” DEM	Ln
NO_ANNA	number of channels	-	VicHydro GIS coverage of Victorian streams	-
K_FACT	soil erosivity	-	ASRIS soil properties mapped at National Scales	-
SED_LOAD	long-term average sediment load	$x10^6$ kg/year	SEDNET output, mostly from National Land and Water Resources Audit results	Ln
SED_CONC	sediment concentration (current catchment condition)	kg/m^3	SEDNET output and mean regulated flow	Ln
RELIEF	catchment relief	-	9” DEM	Ln

Table 3. Parameters derived from regional data sets considered as independent variables for correlation with channel metrics. Cont.

Symbol	Variable	Units	Data Source	Transform*
L_MAX_US	maximum upstream river length	km	Ordered stream network derived from 9" DEM	Sqrt
RAIN	catchment rainfall	mm	ANUCLIM data	Ln
PET_RAIN	ratio of catchment potential evapo-transpiration to rainfall	-	ANUCLIM data	-
R_COEF	runoff coefficient	-	ANUCLIM data and regulated mean flow estimates	Sqrt
QMN_REG	mean flow in the regulated flow regime	m^3/s	regional model based on available streamflow records	Ln
RDSQ_REG	measure of flow variability in the regulated flow regime	-	regional model based on available streamflow records	Ln
MASQ_REG	measure of flow magnitude in the regulated flow regime	-	regional model based on available streamflow records	Ln
QMN_UNR	mean flow in the unregulated flow regime	m^3/s	regional model based on available streamflow records	Ln
MASQ_UNR	measure of flow magnitude in the unregulated flow regime	-	regional model based on available streamflow records	Ln
REG_1.58#	the 1.58 year ARI flood using the partial series for the regulated regime	m^3/s	regional model based on available streamflow records	Ln
UNR_1.58#	the 1.58 year ARI flood using the partial series for the unregulated regime	m^3/s	regional model based on available streamflow records	Ln
R_U_Q1.6	the ratio of regulate to unregulated 1 year ARI flood magnitudes	m^3/s	regional model based on available streamflow records	-
R_U_QMN	the ratio of regulate to unregulated mean flow	m^3/s	regional model based on available streamflow records	-

* Transformation used to normalise the data (dash = no transformation, Ln = natural log transformation, Sqrt = square root transformation)

\# Flow recurrence intervals for 0.5, 1, 2, 5 and 10 years were also estimated using the same procedures.

4.1 Ordered Stream Network

An ordered stream network with a 2 km^2 catchment area threshold was derived from the 9" National DEM for basins across Victoria using parts of the SedNet (Wilkinson *et al.,* 2004) AML code (Streamdefine). The ordered network is a series of stream links connected at nodes. The network is described as "ordered" because the flow direction is known and the downstream link is specified for each node. This means we could follow calculations downstream to accumulate aerial parameters such as catchment area and rainfall. This is the main benefit of the DEM-derived network. Other river network maps such as HYDRO 25, a digitised version of the river network drawn in topographic maps, are not fully ordered (ie. not hydrologically correct) or spatially joined to subcatchment areas so it is not possible to accumulate properties downstream. The 2 km^2 threshold refers to the minimum catchment area (ie. approximating the channel head) for a link to be included in the DEM network.

There are limitations of the DEM-derived network. Firstly, the resolution of the DEM is such that the sinuosity of most of river channels is not fully represented. The river links follow the general alignment of a channel but along a considerably straighter alignment, particularly in lowlands. Secondly, in very flat areas such as the Riverine Plain along the Murray, channel alignment has to be manually specified (edited) since the DEM does not provide a reasonable channel network. Manual entry can mean that channels do not follow the true alignment in very low gradient areas, although topographic maps are used to guide this process. Finally, the upstream boundary of the network is not based on the appearance of formed river channel, but on the artificial threshold of 2 km^2. We know that in dry areas, the DEM-derived network shows low order rivers when in fact no channel exists and vice-versa in wet areas.

The derived river network consisted of approximately 43,000 links with an average length of 2.1 km. Major anabranches were included where necessary. River links were also split at the downstream and upstream end of the 114 reach channel surveys initially collated for the study and river gauging stations.

Strahler network ordering was applied to DEM network (Table 4). The resulting classification is somewhat artificial given the upstream limit of the DEM network is not necessarily consistent with true upstream extent of the channel network. Most of the catchment parameters listed in the table are derived for all links in the stream network, although in some cases, the method used to calculate the parameter could only be applied to a subset of the links.

Channel slope (rise over run between river nodes) was also collected during processing of the DEM. These slopes were adjusted to account for the difference in the sinuosity of the DEM links and the sinuosity indicated in HYDRO25 the statewide digital map of rivers (based on topographic maps). Despite this adjustment they were found to be in considerable error (up to 1-order of magnitude) in comparison to surveyed slopes (particularly for slopes < 0.001) when compared with the bankfull slopes obtained from the hydraulic modelling (discussed in the next Chapter). For this reason, bankfull slopes were used as independent variables in the regression modelling.

Table 4. Total River Length for Streams of Different Order Determined from the DEM-derived Network (note that length are calculated from DEM derived network which underestimates sinuosity).

Strahler Order	Total Length (km)
1	49,300
2	20,600
3	11,300
4	6,070
5	2,700
6	1,860
7	131

Upslope catchment area, percent woody cover (Bureau of Rural Science Land Cover data), mean annual rainfall and PET (ANUCLIM data) were derived by grid analysis and either summed (as with area) or averaged sequentially down through the river network. The parameters are considered accurate to within ± 5%.

4.2 Relief Parameters

A measure of upslope relief was provided by the ratio of the difference between mean and minimum elevations and total range in elevation. Elevations were determined by grid analysis and sequential processing down the river network. The relative relief ratio is considered equivalent to the hypsometric integral. Values typically range from 0.5 or greater for higher relief upstream regions to 0.1 in lowlands with low relief. This is a scale dependant variable depending on position within the river network.

The topographic valley flatness index MrVBF (Gallant and Dowling, 2003) is an expression of local relief in terms of valley confinement and flood plain extent. MrVBF was derived using the 9" DEM. Values typically vary from 2.5 in narrow confined valleys to 8 or higher in broad floodplains. It is also a scale dependant parameter depending on resolution of DEM. The value of MrVBF for each survey reach was derived by averaging the values at the downstream and upstream ends of the reach. The Value of MrVBF was taken to be the maximum value within a 500 m search radius about the survey end points.

4.3 Channel Plan Form Parameters

Channel sinuosity, meander length, and meander radius were determined from the HYDRO25 detailed mapped river network of Victoria. An Arc Macro Language script was written to automate the calculation of plan form geometry throughout river networks. This involves a number of complex geo-processing tasks, but ultimately the average values of these parameters are calculated along river reaches of between 2 and 6 km in length on average. Resultant values for each survey reach were the average of the upstream and downstream ends.

Comparisons between measurements calculated by the AML and those extracted manually in the regions of survey reaches showed a systematic under-prediction of both sinuosity and meander length, although in general there was good correlation between AML measured and manual values ($R^2 > 65\%$). The largest differences occurred for long survey reaches (values at each end were not always representative of the reach as a whole), and where there was significant 2nd order sinuosity. Consequently, in these situations values were manually extracted.

The number of anabranches in the region of the survey reach were also estimated manually by interrogation of the HYDRO25 river network. In most cases the value was one, but along lowland reaches there were occasionally between 2 and 3 anabranches and up to 7 in the most extreme case.

4.4 Bank Resistance

The USLE K-factor (soil erodibility) provides a potential measure of bank resistance to erosion. The K-factor had been previously mapped for the National Land and Water Resources Audit (NLWRA). It is based on ASRIS soil properties (soil texture, permeability rating, organic carbon) mapped at National Scales.

K-factor values were extracted at the upstream and downstream ends of survey reaches and averaged. Values typically vary from 0.017 for less erodible soils to 0.085 for the more erodible soils.

4.5 Hydrological Regionalisation

The hydrological variables include mean annual flow (MAF), the 0.5, 1, 1.5, 2, 5, and 10 year recurrence interval (partial series) flows, and a non-dimensional measure of flow variability - RDSQ (mean of the sum of the ratio between daily flow and mean daily flow raised to power 1.4). River reaches were separated into un-regulated and regulated (e.g., below reservoirs) river reaches for calculating parameters.

Unregulated ('natural') MAF is initially calculated based on regionalisation of the rainfall runoff

coefficient calculated at the network of river gauging stations (Wilkinson *et al.,* in press). This is an interpolation technique based on correlating the mean annual runoff coefficient against the mean annual PET to rainfall ratio (see Appendix II for details). The fitted relationship is used to derive MAF at each link in the river network from upslope catchment area and mean annual rainfall. The mean relative error for observed versus predicted MAF was found to be 30% or better for the seven regions investigated. For regulated reaches, MAF is determined by subtracting the mean annual flow extraction at reservoirs or river off-takes, and applying the same extraction volume down through the river network. Extraction volumes are calculated by comparing gauged MAF to the unregulated prediction of MAF from the above regionalisation.

Flow parameters are first calculated at gauging stations. In general only stations with more than 15 years of continuous flow records were used in the analysis. The time series of daily flows (ML/day) was extracted from the Victorian Data Warehouse and processed using EXCEL macros for MAF and RDSQ.

Partial series flows with ARI > 1 year were calculated by the standard technique specified by Pilgrim (1987): a log-Pearson type 3 (LP3) function was fitted to the n largest independent maximum daily flows (where n = number of years of record). Independence was set at 7 days for peak flows and ARI was calculated from the LP3 (ARI=(nyears+0.2)./(Rank-0.4)). A modified technique was applied to flows with ARI < 1 year because it is not possible to fit LP3 to sub 1-year flows. Instead the *3n* largest independent (same independence criteria) flows were selected, and ARI calculated by linear interpolation rather than LP3.

ARI flows were regionalised across river networks by LLS correlations against MAF and RDSQ. Log space regression coefficients were generally high 0.9 or better for most regions. However, as both MAF and RDSQ are predicted parameters then the mean relative error for predicted versus observed were between 55% and 30% for the 7 regions, suggesting greater uncertainty in predictions.

To help reduce uncertainty, the recurrence interval flow estimates were subsequently adjusted at survey reaches by the local error between observed and predicted flows at the closest gauging stations. In general it was found that flows were being systematically underestimated by some 20 % at most upland sites. In contrast, it was found that flows were typically over-predicted for lowland reaches and this was attributed to anabranch networks becoming active at high flows. Flows were subsequently reduced by 2 and up to 5 fold at some lowland reaches (eg., Wimmera-Loddon and Avon Rivers in particular) based on the degree of anabranching evident both at the site and immediately upstream.

5. Model Development

5.1 Redundancy Analysis for Catchment Parameters

It is not practical to undertake a regression analysis with over 26 independent variables, many of which are cross-correlated. A principle component analysis was used to explore correlations between the parameters. Eight components were extracted and explained 93% of the variance in the parameters. These were adjusted using a Varimax rotation. Variable weights for the rotated components are listed in Table 6.

Table 5. Rotated Component Matrix for Catchment Variables.

	Component							
	1	**2**	**3**	**4**	**5**	**6**	**7**	**8**
C_AREA	0.847	0.448	-0.049	0.177	0.044	0.038	0.077	0.11
MEAND	0.522	-0.043	-0.008	0.071	-0.304	0.02	-0.125	0.729
SIN	0.165	-0.015	-0.022	0.064	0.955	0.027	0.122	-0.126
VBF_MAX	0.534	0.623	-0.146	0.186	0.042	-0.056	0.166	-0.218
USPWC	0.026	-0.855	0.14	0.039	0.071	0.05	-0.008	0.351
RIP_COV	0.01	-0.176	0.131	-0.035	0.028	0.961	-0.073	0.014
CATCH_S	-0.524	-0.773	0.188	-0.16	0.002	-0.004	-0.03	0.025
CATCH_SH	-0.135	-0.219	0.95	0.004	-0.019	0.142	-0.034	0.006
NO_ANNA	0.173	0.073	-0.038	0.11	0.127	-0.075	0.955	-0.065
SED_LOAD	0.674	0.522	0.026	0.016	-0.086	-0.012	0.14	0.097
SED_CONC	-0.102	0.736	0.003	0.032	-0.146	-0.039	0.108	0.094
K_FACT	0.316	0.76	-0.24	0.183	0.063	-0.046	0.147	-0.199
RELIEF	-0.393	-0.671	0.011	-0.217	0.15	-0.196	0.055	0.174
L_MAX_US	0.771	0.429	-0.295	0.17	0.054	0.081	0.077	0.13
RAIN	-0.012	-0.984	0.013	-0.076	-0.005	0.083	0.012	-0.062
PET_RAIN	0.044	0.97	0.001	0.134	0.012	-0.001	0.068	-0.011
R_COEF	-0.09	-0.916	0.048	-0.047	-0.01	0.053	-0.004	-0.254
QMN_REG	0.98	-0.089	0.03	-0.013	0.04	0.025	0.069	0.028
RDSQ_REG	-0.044	0.948	-0.071	0.057	0.071	-0.184	-0.029	0.072
MASQ_REG	0.987	-0.019	0.011	-0.061	0.034	0.009	0.041	0.032
QMN_UNR	0.97	-0.045	-0.029	0.162	0.05	0.071	0.086	0.01
MASQ_UNR	0.969	0.056	-0.036	0.169	0.058	0.051	0.083	0.018
REG_UNR	-0.205	-0.372	0	-0.877	-0.08	0.049	-0.141	-0.049
SLOPE	-0.557	-0.413	0.109	-0.083	-0.075	0.167	-0.084	-0.048
UNR_1.58	0.937	0.185	-0.086	0.155	0.048	-0.077	0.002	0.07
REG_1.58	0.951	0.054	-0.086	-0.152	0.032	-0.114	-0.026	0.055
C_AREA	0.847	0.448	-0.049	0.177	0.044	0.038	0.077	0.11
MEAND	0.522	-0.043	-0.008	0.071	-0.304	0.02	-0.125	0.729
SIN	0.165	-0.015	-0.022	0.064	0.955	0.027	0.122	-0.126
VBF_MAX	0.534	0.623	-0.146	0.186	0.042	-0.056	0.166	-0.218
USPWC	0.026	-0.855	0.14	0.039	0.071	0.05	-0.008	0.351
RIP_COV	0.01	-0.176	0.131	-0.035	0.028	0.961	-0.073	0.014
CATCH_S	-0.524	-0.773	0.188	-0.16	0.002	-0.004	-0.03	0.025
CATCH_SH	-0.135	-0.219	0.95	0.004	-0.019	0.142	-0.034	0.006
NO_ANNA	0.173	0.073	-0.038	0.11	0.127	-0.075	0.955	-0.065
SED_LOAD	0.674	0.522	0.026	0.016	-0.086	-0.012	0.14	0.097
SED_CONC	-0.102	0.736	0.003	0.032	-0.146	-0.039	0.108	0.094

We chose not use the principle components as our independent variables because they complicate interpretation of results and require considerable data for calculation. Instead we chose an initial set of three variables (Q1.58_UNR, BF_SLOPE and SED_CONC) because theoretical considerations and existing empirical models of channel metrics support their geomorphic importance. We then chose 7 additional variables based on the strength of correlation with the un-selected parameters. In other words, the variables were chosen to maximise correlations between the 27 variables and the sub-set of 10 selected variables. The selected variables are listed as GROUP 1 in Table 6. With the exception of BF_SLOPE and SEDCONC, these parameters are variables with the highest weighting for each principle component in Table 6. We also use a second group of independent variables which are identical to the first group except the regulated 1.58 year flood is used instead of the unregulated (GROUP 2 in Table 6).

In some cases it may not be possible to calculate the UNR_1.58 (1.58 year flood in the unregulated regime), REG_1.59 and SED_CONC (sediment concentration, which was estimated using SEDNET in our case). For this reason, we re-selected 10 independent variables using the same procedure but omitting these two and pre-selecting the mean unregulated flow (GROUP 3 in Table 6). In some cases, not even the mean unregulated flow will be available so we repeated the variable selection, omitting this variable (GROUP 4 in Table 6). In some cases it may be quite easy to obtain estimates of bankfull width in the field or from air photos, so we also selected a set of 10 independent variables from all those available with the addition of bankfull width (GROUP 5 in Table 6). Finally, we selected a set of 10 variables, pre-selecting the bankfull discharge as the initial variable (GROUP 6 in Table 6).

Table 6. The Six Groups of Independent Variables using Multivariate Regression Analysis.

GROUP 1 Selected from full set of available variables	**GROUP 2** Selected from full set of available variables (using reg. flow mag)	**GROUP 3** Using mean discharge (excluding SED_CONC and UNR_1.58)	**GROUP 4** Using catchment area *(Excluding QMN_UNR, SED_CONC and UNR_1.58)*	**GROUP 5** All variables with the addition of Bankfull Width	**GROUP 6** Using bankfull discharge (Q_{bf})
UNR_1.58*	REG_1.58*	QMN_UNR*	C_AREA*	BF_W*	Q_BF*
SLOPE*	SLOPE*	CATCH_S	RAIN*	SLOPE*	CATCH_S
SED_CONC*	SED_CONC*	MEAND	PET_RAIN*	SED_CONC*	SIN
PET_RAIN	PET_RAIN	RIP_COV	SIN	CATCH_S	RAIN
NO_ANNA	NO_ANNA	CATCH_SH	CATCH_SH	QMN_UNR	RIP_COV
RIP_COV	RIP_COV	NO_ANNA	NO_ANNA	SIN	NO_ANNA
CATCH_SH	CATCH_SH	SIN	RIP_COV	RIP_COV	CATCH_SH
SIN	SIN	R_U_QMN*	MEAND	R_U_QMN	MEAND
R_U_Q1.6	R_U_Q1.6	SLOPE	SLOPE	CATCH_SH	SED_CONC
MEAND	MEAND	USPWC	RELIEF	NO_ANNA	SLOPE

* Variables selected before the redundancy analysis because of their obvious geomorphic significance

5.2 Bankfull Width

We undertook a step-wise multi-variate linear regression to correlate the bankfull dimensions with the 10 independent variables selected in the previous section. We developed linear models for the mean and standard deviation of bankfull width (W_{bf}) and mean depth (D_{bf} = cross-section area divided by top width). The resulting equations are given on the following pages. In most cases these can be expressed as power functions since logarithmic transformations were used for all the selected variables. A selection of equations is given for dimensions where additional variables could explain a significant proportion of the variance. Equations are reported for regressions carried out using each of the 6 groups of independent variables listed in Table 6. Plots of the observed and modelled values corresponding to the following regression equations are given in Appendix III.

GROUP 1

$$\overline{W}_{bf} = 5.60(\text{UNR\_1.58})^{0.383} \qquad r^2 = 0.71,\ E = 0.35,\ M1.$$

$$\overline{W}_{bf} = 1.93(\text{UNR\_1.58})^{0.329}(\text{MEAND})^{0.213} \qquad r^2 = 0.75,\ E = 0.33,\ M2.$$

$$\overline{W}_{bf} = 1.48(\text{UNR\_1.58})^{0.279}(\text{MEAND})^{0.224}(\text{SLOPE})^{-0.063} \qquad r^2 = 0.76,\ E = 0.32,\ M3.$$

GROUP 2

$$\overline{W}_{bf} = 6.44(\text{REG\_1.58})^{0.379} \qquad r^2 = 0.62,\ E = 0.40,\ M4.$$

$$\overline{W}_{bf} = 5.54(\text{REG\_1.58})^{0.388}(\text{R\_U1.5})^{-0..347} \qquad r^2 = 0.71,\ E = 0.35,\ M5.$$

$$\overline{W}_{bf} = 1.93(\text{REG\_1.58})^{0.332}(\text{R\_U1.5})^{-0.316}(\text{MEAND})^{0.212} \qquad r^2 = 0.75,\ E = 0.33,\ M6.$$

$$\overline{W}_{bf} = 2.25(\text{REG\_1.58})^{0.338}(\text{R\_U1.5})^{-0.263}(\text{MEAND})^{0.205}(\text{SED\_CONC})^{0.051} \qquad r^2 = 0.76,\ E = 0.32,\ M7.$$

GROUP 3

$$\overline{W}_{bf} = 18.6(\text{QMN\_UNR})^{0.330} \qquad r^2 = 0.60,\ E = 0.41,\ M8.$$

$$\overline{W}_{bf} = 3.59(\text{QMN\_UNR})^{0.270}(\text{MEAND})^{0.284} \qquad r^2 = 0.68,\ E = 0.37,\ M9.$$

$$\overline{W}_{bf} = 1.93(\text{QMN\_UNR})^{0.201}(\text{MEAND})^{0.278}(\text{SLOPE})^{-0.112} \qquad r^2 = 0.72,\ E = 0.34,\ M10.$$

GROUP 4

$$\overline{W}_{bf} = 4.01(\text{C\_AREA})^{0.291} \qquad r^2 = 0.65,\ E = 0.39,\ M11.$$

$$\overline{W}_{bf} = 1.05(\text{C\_AREA})^{0.243}(\text{MEAND})^{0.274} \qquad r^2 = 0.72,\ E = 0.34,\ M12.$$

$$\overline{W}_{bf} = 1.52(\text{C\_AREA})^{0.292}(\text{MEAND})^{0.216}e^{-0.239.\text{PET\_RAIN}} \qquad r^2 = 0.75,\ E = 0.33,\ M13.$$

GROUP 5: *Not applicable because bankfull width cannot be treated as an independent variable.*

GROUP 6

$$\overline{W}_{bf} = 4.63(\text{Q}_{bf})^{0.428} \qquad r^2 = 0.78,\ E = 0.31,\ M14.$$

$$\overline{W}_{bf} = 2.42(\text{Q}_{bf})^{0.361}(\text{SLOPE})^{-0.139} \qquad r^2 = 0.88,\ E = 0.23,\ M15.$$

$$\overline{W}_{bf} = 1.51(\text{Q}_{bf})^{0.331}(\text{SLOPE})^{-0.136}(\text{MEAND})^{0.102} \qquad r^2 = 0.89,\ E = 0.22,\ M16.$$

5.3 Mean Bankfull Depth

GROUP 1

$$\overline{D}_{bf} = 0.553(\text{UNR\_1.58})^{0.330} \qquad r^2 = 0.68, \text{E} = 0.33, \text{M17}.$$

$$\overline{D}_{bf} = 0.533(\text{UNR\_1.58})^{0.348}(\text{R\_U\_Q1.5})^{0.139} \qquad r^2 = 0.69, \text{E} = 0.32, \text{M18}.$$

GROUP 2

$$\overline{D}_{bf} = 0.584(\text{REG\_1.58})^{0.342} \qquad r^2 = 0.65, \text{E} = 0.34, \text{M19}.$$

$$\overline{D}_{bf} = 0.533(\text{REG\_1.58})^{0.348}(\text{R\_U\_Q1.5})^{-0.209} \qquad r^2 = 0.69, \text{E} = 0.32, \text{M20}.$$

GROUP 3

$$\overline{D}_{bf} = 1.55(\text{QMN\_UNR})^{0.287} \qquad r^2 = 0.58, \text{E} = 0.37, \text{M21}.$$

$$\overline{D}_{bf} = 1.73(\text{QMN\_UNR})^{0.305} e^{-0.097.\text{NO\_ANNA}} \qquad r^2 = 0.60, \text{E} = 0.37, \text{M22}.$$

$$\overline{D}_{bf} = 1.14(\text{QMN\_UNR})^{0.261}(\text{SLOPE})^{-0.073} e^{-0.105.\text{NO\_ANNA}} \qquad r^2 = 0.62, \text{E} = 0.35, \text{M23}.$$

GROUP 4

$$\overline{D}_{bf} = 0.470(\text{C\_AREA})^{0.233} \qquad r^2 = 0.54, \text{E} = 0.39, \text{M24}.$$

$$\overline{D}_{bf} = 0.529(\text{C\_AREA})^{0.286} e^{-0.327.\text{PET\_RAIN}} \qquad r^2 = 0.60, \text{E} = 0.36, \text{M25}.$$

$$\overline{D}_{bf} = 0.550(\text{C\_AREA})^{0.301} e^{-(0.336.\text{PET\_RAIN}+0.093.\text{NO\_ANNA})} \qquad r^2 = 0.62, \text{E} = 0.36, \text{M26}.$$

GROUP 5

$$\overline{D}_{bf} = 0.209(\text{W}_{bf})^{0.714} \qquad r^2 = 0.65, \text{E} = 0.34, \text{M27}.$$

$$\overline{D}_{bf} = 0.381(\text{W}_{bf})^{0.480}(\text{QMN\_UNR})^{0.128} \qquad r^2 = 0.70, \text{E} = 0.32, \text{M28}.$$

GROUP 6

$$\overline{D}_{bf} = 0.413(\text{Q}_{bf})^{0.396} \qquad r^2 = 0.87, \text{E} = 0.21, \text{M29}.$$

$$\overline{D}_{bf} = 0.278(\text{Q}_{bf})^{0.356}(\text{SLOPE})^{-0.085} \qquad r^2 = 0.91, \text{E} = 0.17, \text{M30}.$$

$$\overline{D}_{bf} = 0.403(\text{Q}_{bf})^{0.379}(\text{SLOPE})^{-0.087}(\text{MEAND})^{-0.080} \qquad r^2 = 0.92, \text{E} = 0.16, \text{M31}.$$

5.4 Bankfull Discharge

GROUP 1

$$Q_{bf} = 3.16(\text{UNR\_1.58})^{0.740} \qquad r^2 = 0.62, \text{E} = 0.84, \text{M32}.$$

$$Q_{bf} = 0.348(\text{UNR\_1.58})^{0.629}(\text{MEAND})^{0.441} \qquad r^2 = 0.66, \text{E} = 0.79, \text{M33}.$$

$$Q_{bf} = 0.772(\text{UNR\_1.58})^{0.779}(\text{MEAND})^{0.409}(\text{SLOPE})^{0.188} \qquad r^2 = 0.68, \text{E} = 0.77, \text{M34}.$$

GROUP 2

$$Q_{bf} = 3.45(\text{REG\_1.58})^{0.776} \qquad r^2 = 0.61, \text{E} = 0.85, \text{M35}.$$

$$Q_{bf} = 0.347(\text{REG\_1.58})^{0.656}(\text{MEAND})^{0.456} \qquad r^2 = 0.65, \text{E} = 0.80, \text{M36}.$$

$$Q_{bf} = 0.367(\text{REG\_1.58})^{0.677}(\text{MEAND})^{0.414}(\text{R\_U\_Q1.5})^{-0.360} \qquad r^2 = 0.67, \text{E} = 0.78, \text{M37}.$$

$$Q_{bf} = 0.760(\text{REG\_1.58})^{0.809}(\text{MEAND})^{0.388}(\text{R\_U\_Q1.5})^{-0.538}(\text{SLOPE})^{0.173} \qquad r^2 = 0.69, \text{E} = 0.76, \text{M38}.$$

GROUP 3

$$Q_{bf} = 31.7(\text{QMN\_UNR})^{0.648} \qquad r^2 = 0.54, \text{E} = 0.92, \text{M39}.$$

$$Q_{bf} = 1.21(\text{QMN\_UNR})^{0.529}(\text{MEAND})^{0.564} \qquad r^2 = 0.61, \text{E} = 0.85, \text{M40}.$$

GROUP 4

$$Q_{bf} = 2.50(\text{C\_AREA})^{0.504} \qquad r^2 = 0.45, \text{E} = 1.00, \text{M41}.$$

$$Q_{bf} = 3.60(\text{C\_AREA})^{0.666} e^{-0.999.\text{PET\_RAIN}} \qquad r^2 = 0.57, \text{E} = 0.89, \text{M42}.$$

$$Q_{bf} = 0.380(\text{C\_AREA})^{0.554}(\text{MEAND})^{0.444} e^{-0.790.\text{PET\_RAIN}} \qquad r^2 = 0.61, \text{E} = 0.85, \text{M43}.$$

GROUP 5

$$Q_{bf} = 0.158(\text{W}_{bf})^{1.84} \qquad r^2 = 0.78, \text{E} = 0.63, \text{M44}.$$

$$Q_{bf} = 0.218(\text{W}_{bf})^{2.22}(\text{SLOPE})^{0.240} \qquad r^2 = 0.83, \text{E} = 0.56, \text{M45}.$$

$$Q_{bf} = 0.504(\text{W}_{bf})^{1.95}(\text{SLOPE})^{0.266}(\text{QMN\_UNR})^{0.171} \qquad r^2 = 0.84, \text{E} = 0.54, \text{M46}.$$

GROUP 6: *Not applicable since bankfull discharge cannot be treated as an independent variable.*

OTHER

$$Q_{bf} = 12.6(\text{D}_{bf})^{2.19} \qquad r^2 = 0.87, \text{E} = 0.49, \text{M47}.$$

$$Q_{bf} = 1.57(\text{D}_{bf})^{1.46}(\text{W}_{bf})^{0.791} \qquad r^2 = 0.92, \text{E} = 0.39, \text{M48}.$$

$$Q_{bf} = 2.82(\text{D}_{bf})^{1.59}(\text{W}_{bf})^{1.17}(\text{SLOPE})^{0.291} \qquad r^2 = 0.99, \text{E} = 0.15, \text{M49}.$$

$$Q_{bf} = 4.81(\text{Dmax}_{bf})^{2.14} \qquad r^2 = 0.84, \text{E} = 0.54, \text{M50}.$$

$$Q_{bf} = 0.777(\text{Dmax}_{bf})^{1.37}(\text{W}_{bf})^{0.834} \qquad r^2 = 0.89, \text{E} = 0.45, \text{M51}.$$

$$Q_{bf} = 1.48(\text{Dmax}_{bf})^{1.57}(\text{W}_{bf})^{1.18}(\text{SLOPE})^{0.310} \qquad r^2 = 0.97, \text{E} = 0.23, \text{M52}.$$

5.5 Channel Slope

In the following regression equations (and all others) SLOPE refers to the reach energy slope at bankfull discharge estimated from water levels modelled for each reach. The parameter DEM_S is the slope derived from digital elevation model and adjusted using the true sinuosity calculated from the river courses shown on the 1:25000 topographic maps which are available in digital form.

$$\mathrm{SLOPE} = 0.129e^{-(0.815.\mathrm{VBF\_MAX})} \qquad r^2 = 0.54,\ \mathrm{E} = 1.09,\ \mathrm{M53}.$$

$$\mathrm{SLOPE} = 0.165(\mathrm{UNR\_1.58})^{-0.378} e^{-(0.566.\mathrm{VBF\_MAX})} \qquad r^2 = 0.60,\ \mathrm{E} = 1.02,\ \mathrm{M54}.$$

$$\mathrm{SLOPE} = 0.208(\mathrm{UNR\_1.58})^{-0.349} (\mathrm{DEM\_S})^{0.126} e^{-(0.473.\mathrm{VBF\_MAX})} \qquad r^2 = 0.62,\ \mathrm{E} = 1.00,\ \mathrm{M55}.$$

$$\mathrm{SLOPE} = 0.106(\mathrm{UNR\_1.58})^{-0.355} (\mathrm{DEM\_S})^{0.144} e^{(0.955.\mathrm{RIP\_COV}-0.413.\mathrm{VBF\_MAX})} \qquad r^2 = 0.64,\ \mathrm{E} = 0.97,\ \mathrm{M56}.$$

5.6 Channel Shape

using group 1 independent variables

Width to Depth Ratio

$$\frac{\mathrm{W_{bf}}}{\mathrm{D_{bf}}} = 4.77(\mathrm{MEAND})^{0.162} \qquad r^2 = 0.08,\ \mathrm{E} = 0.37,\ \mathrm{M57}.$$

Wetted Perimeter to Width Ratio

$$\frac{\mathrm{P_{bf}}}{\mathrm{W_{bf}}} = 1.21(\mathrm{MEAND})^{-0.019} \qquad r^2 = 0.15,\ \mathrm{E} = 0.03,\ \mathrm{M58}.$$

$$\frac{\mathrm{P_{bf}}}{\mathrm{W_{bf}}} = 1.23(\mathrm{MEAND})^{-0.016} (\mathrm{SLOPE})^{0.006} \qquad r^2 = 0.22,\ \mathrm{E} = 0.03,\ \mathrm{M59}.$$

Maximum Depth to Mean Depth Ratio

$$\frac{\mathrm{Dmax_{bf}}}{\mathrm{D_{bf}}} = 1.38e^{(0.093.\mathrm{PET\_RAIN})} \qquad r^2 = 0.17,\ \mathrm{E} = 0.11,\ \mathrm{M60}.$$

$$\frac{\mathrm{Dmax_{bf}}}{\mathrm{D_{bf}}} = 1.86(\mathrm{MEAND})^{-0.048} e^{(0.091.\mathrm{PET\_RAIN})} \qquad r^2 = 0.25,\ \mathrm{E} = 0.10,\ \mathrm{M61}.$$

Standard Deviation of Width

No model

Standard Deviation of Mean Depth

$$\sigma_{\mathrm{D\_bf}} = 0.025.\ln(\mathrm{SLOPE}) + 0.373 \qquad r^2 = 0.10,\ \mathrm{E} = 0.12,\ \mathrm{M62}.$$

5.7 At-A-Station Hydraulic Geometry Parameters

The basic at-a-station hydraulic geometry equations for width have two-parts

$$W = a_1 Q^{b1}, \qquad Q \le Q_{cp}$$

$$W = a_2 Q^{b2}, \qquad Q > Q_{cp}$$

Instead of the 4 parameters in these equations, we use transformation proposed by Bates (1990) θ_{W2}, θ_{W3}, Q_{cp} and a_2 *where:*

$$\theta_{w2} = (b_1 + b_2) / 2$$

$$\theta_{w3} = (b_2 - b_1) / 2$$

Equations can be rearranged to give

$$b_1 = \theta w_2 - \theta w_3$$

$$b_2 = \theta w_2 + \theta w_3$$

$$a_1 = a_2 Q_{cp}^{2\theta_{w3}}$$

Likewise for mean depth except coefficient and exponent are denoted by c_i and f_i respectively.

GROUP 1

$Q_{cp} = 2.38(\text{UNR\_1.58})^{0.277}$ — r^2 = 0.21, E = 0.77, M63.

$Q_{cp} = 3.94(\text{UNR\_1.58})^{0.389}(\text{SLOPE})^{0.148}$ — r^2 = 0.24, E = 0.75, M64.

$\theta_{W2} = 0.014.\ln(\text{SED\_CONC}) + 0.270$ — r^2 = 0.08, E = 0.076, M65.

$\theta_{W3} = -0.025.\ln(\text{MEAND}) + 0.162$ — r^2 = 0.06, E = 0.064, M66.

$a_2 = 0.409(\text{MEAND})^{0.530}$ — r^2 = 0.33, E = 0.55, M67.

$a_2 = 0.537(\text{MEAND})^{0.356}(\text{UNR\_1.58})^{0.175}$ — r^2 = 0.43, E = 0.51, M68.

$\theta_{D2} = -0.060(\text{PET\_RAIN}) + 0.505$ — r^2 = 0.15, E = 0.075, M69.

$\theta_{D2} = -0.051(\text{PET\_RAIN}) - 0.013.\ln(\text{UNR\_1.58}) + 0.551$ — r^2 = 0.20, E = 0.074, M70.

$\theta_{D3} = 0.032.\ln(\text{MEAND}) - 0.160$ — r^2 = 0.12, E = 0.060, M71.

$c_2 = 0.206e^{0.330.\text{PET\_RAIN}}$ — r^2 = 0.14, E = 0.43, M72.

$c_2 = 0.865e^{0.323.\text{PET\_RAIN}}(\text{MEAND})^{-0.232}$ — r^2 = 0.27, E = 0.40, M73.

GROUP 2

$Q_{cp} = 2.38(\text{REG\_1.58})^{0.298}$ r^2 = 0.22, E = 0.76, M74.

θ_{W2} model is the same as for Group 1

θ_{W3} model is the same as for Group 1

$a_2 = 0.409(\text{MEAND})^{0.530}$ (as for Group 1) r^2 = 0.33, E = 0.55, M75.

$a_2 = 0.278(\text{MEAND})^{0.450}(\text{SLOPE})^{-0.128}$ r^2 = 0.41, E = 0.52, M76.

$a_2 = 0.207(\text{MEAND})^{0.442}(\text{SLOPE})^{-0.150}(\text{SED\_CONC})^{-0.081}$ r^2 = 0.44, E = 0.50, M77.

$\theta_{D2} = -0.060(\text{PET\_RAIN}) + 0.505$ (as for Group 1) r^2 = 0.15, E = 0.075, M78.

$\theta_{D2} = -0.054(\text{PET\_RAIN}) + 0.025.\ln(\text{CATCH\_SH}) + 0.544$ r^2 = 0.19, E = 0.074, M79.

θ_{D3} model is the same as for Group 1

C_2 model is the same as for Group 1

GROUP 3

$Q_{cp} = 5.76(\text{QMN\_UNR})^{0.229}$ r^2 = 0.17, E = 0.79, M80.

$Q_{cp} = 1.11(\text{QMN\_UNR})^{0.169}(\text{MEAND})^{0.283}$ r^2 = 0.20, E = 0.77, M81.

No model for θ_{W2}.

θ_{W3} model is the same as for Group 1

$a_2 = 7.04(\text{QMN\_UNR})^{0.252}$ r^2 = 0.33, E = 0.55, M82.

$a_2 = 0.855(\text{QMN\_UNR})^{0.175}(\text{MEAND})^{0.364}$ r^2 = 0.45, E = 0.50, M83.

$\theta_{D2} = 0.031.\ln(\text{CATCH\_S}) + 0.600$ r^2 = 0.22, E = 0.073, M84.

$\theta_{D3} = 0.032.\ln(\text{MEAND}) - 0.160$ (as for Group 1) r^2 = 0.12, E = 0.060, M85.

$\theta_{D3} = 0.023.\ln(\text{MEAND}) + 0.009.\ln(\text{QMN\_UNR}) - 0.122$ r^2 = 0.15, E = 0.060, M86.

$c_2 = 1.46(\text{MEAND})^{-0.238}$ r^2 = 0.13, E = 0.44, M87.

$c_2 = 0.847(\text{MEAND})^{-0.300}(\text{CATCH\_S})^{-0.155}$ r^2 = 0.28, E = 0.40, M88.

GROUP 4

$$Q_{cp} = .548(\text{MEAND})^{0.444}$$ r^2 = 0.13, E = 0.80, M89.

$$Q_{cp} = 0.522(\text{MEAND})^{0.311}(\text{C\_AREA})^{0.121}$$ r^2 = 0.18, E = 0.78, M90.

$$\theta_{W2} = -0.038(\text{PET\_RAIN}) + 0.177$$ r^2 = 0.06, E = 0.077, M91.

θ_{W3} model is the same as for Group 1

$$a_2 = 0.409(\text{MEAND})^{0.530}$$ (as for Group 1) r^2 = 0.33, E = 0.55, M92.

$$a_2 = 0.389(\text{MEAND})^{0.396}(\text{C\_AREA})^{0.122}$$ r^2 = 0.41, E = 0.51, M93.

$$a_2 = 0.691(\text{MEAND})^{0.307}(\text{C\_AREA})^{0.198}\text{e}^{-0.369.\text{PET\_RAIN}}$$ r^2 = 0.46, E = 0.49, M94.

$$\theta_{D2} = 0.101.\ln(\text{RAIN}) - 0.263$$ r^2 = 0.17, E = 0.075, M95.

$$\theta_{D2} = \ln(\text{RAIN}^{0.068}\text{C\_AREA}^{-0.012}) + 0.040$$ r^2 = 0.21, E = 0.073, M96.

Models for θ_{D3} as for Group 1

$$c_2 = 0.206e^{0.330.\text{PET\_RAIN}}$$ r^2 = 0.14, E = 0.43, M97.

$$c_2 = 0.865e^{0.323.\text{PET\_RAIN}}(\text{MEAND})^{-0.232}$$ r^2 = 0.27, E = 0.40, M98.

GROUP 5

$$Q_{cp} = 0.538(\text{W}_{\text{bf}})^{0.792}$$ r^2 = 0.36, E = 0.69, M99.

$$Q_{cp} = 0.707(\text{W}_{\text{bf}})^{1.11}(\text{SLOPE})^{0.202}$$ r^2 = 0.43, E = 0.65, M100.

Models for θ_{W2} as for Group 1

No model for θ_{W3}.

$$a_2 = 1.12(\text{W}_{\text{bf}})^{0.651}$$ r^2 = 0.40, E = 0.52, M101.

$$a_2 = 0.841(\text{W}_{\text{bf}})^{0.679}(\text{SED\_CONC})^{-0.077}$$ r^2 = 0.43, E = 0.51, M102.

Models for θ_{D2} as for Group 3

$$\theta_{D3} = 0.014.\ln(\text{QMN\_UNR}) + 0.011$$ r^2 = 0.10, E = 0.06, M103.

$$c_2 = 0.171(\text{CATCH\_S})^{-0.114}$$ r^2 = 0.083, E = 0.45, M104.

$$c_2 = 0.290(\text{CATCH\_S})^{-0.208}(\text{W}_{\text{bf}})^{-0.316}$$ r^2 = 0.21, E = 0.42, M105.

GROUP 6

$Q_{cp} = 1.08(Q_{bf})^{0.453}$ r^2 = 0.50, E = 0.61, M106.

Models for θ_{W2} as for Group 1

Models for θ_{W3} as for Group 1

Models for a_2 as for Group 2

Models for θ_{D2} as for Group 3

Models for θ_{D3} as for Group 1

Models for c_2 as for Group 3

6. Discussion

6.1 Channel Dimensions

As is widely reported in the literature bankfull width and depth are strongly correlated with flow magnitude regardless of the flow statistic used. For the case of bankfull width, the unregulated 1.58 year flood was the most strongly correlated parameter considered. We subsequently confirmed that the 1.58 year unregulated flood magnitude was the most strongly correlated flood statistic of all those calculated using the hydrological regionalisation. For bankfull depth, a combination of the unregulated and regulated 1.58 year flood magnitude provided the strongest correlation of those considered. Any effect of river regulation on bankfull width is not detected in this analysis. In contrast, there is a consistent trend of reduced bankfull depth where the magnitude of more frequent floods has been reduced through regulation. Catchment area and mean flow explained less variance in channel dimensions than the flood statistics.

Generally bankfull width increased with meander wavelength but bankfull depth showed no such trend. This could simply be a consequence of scaling with larger rivers having larger meander wavelengths although the lack of relation with depth does not support this explanation. Alternatively, meander wavelength may be a surrogate measure for bank erosion resistance. Other studies have suggested that increased erosion resistance of stream banks (through increased clay content or resistance of bank vegetation) is generally associated with reduced width to depth ratios. Increased meander wavelength (for the same bend amplitude) means a greater radius of curvature around meander bends which tends to reduce maximum shear stress on the outside of meander bends. The cross-section form ratio (i.e. bankfull width divided by depth) generally increases with meander wavelength supporting the notion that meander wavelength is a surrogate measure of bank strength.

Channel gradient was a less important variable in the regression models for explaining variation in channel dimensions. There is some indication that channels are smaller in higher gradient streams of similar catchment size or with a similar bankfull discharge. However, with cross correlation between channel slope, catchment area and flow magnitude, it is not possible to distinguish the effect of slope.

Relations between bankfull width and depth suggest that larger channels tend to have larger width to depth ratios. However, closer examination of downstream trends (not included in this report) for most rivers show the W/D ratio either remains constant or decreases with distance downstream. Indeed, it seems that bankfull width raised to the power of 0.71 divided by mean depth is a scale-independent ratio with an average value of 4.8. Flow regulation which seems to slightly reduce bankfull depths may have an influence on this result although degree of regulation didn't explain any additional variance.

Regression models of bankfull width and depth using bankfull discharge and channel slope as independent variables have a very high correlation coefficient (r^2=0.88 and r^2=0.91 respectively for log transformed variables). However some of this correlation may be spurious as a consequence of bankfull discharge being estimated using bankfull width and depth.

Unexplained variance, even with the best models of bankfull dimensions using the regulated and unregulated 1.58 year floods, is an order of magnitude greater than uncertainty in the estimates of channel dimensions derived from the channel surveys (Table 2). This means that unexplained variance is not solely a consequence of random errors in estimates of the hydraulic metrics. Some error in the independent variables is also to be expected (in particular the flood magnitude) and will reduce the correlation coefficients in these regression equations. One might expect that uncertainty in the flood magnitudes is responsible for at least 10% of variance in the estimated (log-transformed) flood magnitudes. A 10% error in the independent variable of a simple regression equation will reduce the correlation coefficient by 10%. We might expect a reasonable proportion, but not all, of the unexplained variance is a consequence of errors in estimates of flood magnitudes. Any remaining

variance after allowing for uncertainties in the dependent and independent variables is small (less than 20%). Explaining this remaining variance in bankfull dimensions may be difficult using this data set which includes a very broad range of sites and survey designs.

Increasing random errors in the independent variables of a linear regression equation tends to reduce the resulting gradients (i.e. the exponent in power functions produced by log-log regressions) but the intercepts (i.e. the power function coefficients) are unaffected. Our simple log-log regressions of width and depth with the unregulated flood magnitudes give exponents of 0.38 and 0.33. If we knew the magnitude of these errors we could adjust these exponents to obtain unbiased estimates. This is particularly so, since the error in discharge is likely to have increased with distance downstream as there were few unregulated gauges stations in lowlands from which to constrain the flow regionalisations, and estimates in lowland reaches largely relied on extrapolation and are probably overestimates due to flow loss along the multiple anabranching and cutoffs on most rivers. It is expected that further investigations of these relations using more precise estimates of flood magnitudes would produce higher exponents for these terms. The exponents are in reality likely closer to those for bankfull discharge (0.43 and 0.40). Given these errors are unknown our recommendation is to use the regression equations as reported.

We can estimate the maximum possible values for the exponents in our simple linear regressions with the 1.58 year unregulated flood magnitude. The maximum random error in the 1.58 year flood magnitudes is 0.6 (standard error in the log-transformed 1.58 year unregulated flood magnitude). This is equivalent to 17% of the observed variance in the log-transformed flood magnitude. This is calculated by assuming all unexplained variance in the regression equations using the Group 1 independent variables is due to random errors calculated in the dependent variables (Table 2) and errors in the estimated flood magnitude. Each regression equation thus provides an estimate of the error in the flood magnitude estimates. The minimum error estimated for each regression equation is the upper limit for the actual error. Effectively, the correlation coefficients for our regression equations would not be possible if errors in flood magnitude were larger than 0.6. If this was the actual error in the flood magnitude, the maximum possible exponents are 0.46 and 0.39 for the simple linear regressions for bankfull width and depth respectively with the 1.58 year unregulated flood magnitude. However standard error in the flood magnitude can be less than 0.6 and the correct exponents will be somewhere between our values (0.38 and 0.33 for width and depth respectively) and these maximum values. The picture is more complicated with the multivariate relations.

6.2 Bankfull Discharge

It is no surprise that bankfull discharge increases with magnitude of the 1.58 year flood magnitude. Indeed this flood magnitude has been used to estimate bankfull discharge based on empirical results in some regions of the Unites States. At a 1.58 year flood magnitude of 84 m^3/s (or 7,200 Ml/day) the simple regression equation relating this flood magnitude to bankfull discharge gives the same magnitude for bankfull discharge. The bankfull discharge is generally less than this flood magnitude with increasing flood magnitudes greater than 84 m^3/s and greater than the 1.58 year flood magnitude with decreasing flood magnitudes. In other words, smaller catchments generally have larger channels relative to flood magnitude of a given recurrence interval and the frequency of the bankfull flow tends to increase with increasing catchment area.

We should remember that random errors in our estimate of the unregulated 1.58 year flood magnitude will tend to reduce the exponent for the log-log regressions. Assuming a maximum error in the flood magnitude is 0.6 than the maximum unbiased estimate of the exponent in the simple log-log regression between bankfull discharge and the 1.58 year unregulated flood magnitude is 0.89. The coefficient is not biased by such random errors, which suggests that bankfull discharge is on average somewhat larger than the 1.58 year flood for rivers across Victoria. This is also true given the likely overestimate of flood

discharge in lowlands which would further increase the value of the exponent.

It is interesting that bankfull discharge generally increases with increasing meander wavelength. If meander wavelength is a surrogate measure of bank erosivity (as discussed earlier) then channels with more resistant banks will have a smaller bankfull discharge, all else being equal.

Regression results suggest that 66% of the variance in bankfull discharge can be estimated by the 1.58 year unregulated flood magnitude and meander wavelength. A further 4% of the variance in bankfull discharge is due to random errors associated with the hydraulic surveys and modelling. Of the remaining unexplained variance apparent in the regression results, up to 10% may be a consequence of errors in estimating the independent variables in particular the 1.58 year unregulated flood magnitude. This leaves at least 20% of the variance in bankfull discharge.

The simple log-log regression relating bankfull discharge to width has a coefficient of determination of 0.78. We estimated standard errors in log-transformed bankfull discharge and width to be 0.23 and 0.14. These errors will tend to reduce the observed correlation coefficients. There is also potential for some observed correlation to be spurious because bankfull width is used to calculate bankfull discharge. Spurious correlation is introduced into the relation because the random errors for the two dependent and independent variables may be correlated. Some of the observed correlation may be a consequence of correlated error terms. We used a numerical procedure to account for the effects of random errors assuming that the errors in bankfull discharge are entirely a consequence of errors in estimates of bankfull width. This is an extreme assumption since much of the error in bankfull discharge will be associated with errors in other variables including channel slope and roughness. However using this assumption we found that errors including effects of spurious correlation are sufficiently small to be neglected. Using a numerical analysis we find that bias correction to account for these errors had very little effect on the resulting coefficients and correlation.

This result suggests that where precise bankfull width estimates are available, bankfull discharge is more accurately estimated using a simple log-log regression equation with bankfull width than the estimated 1.58 year flood magnitude. This is a useful result since bankfull width estimates are relatively easy to measure in the field and can also be estimated from remotely sensed data such air photos, very high resolution satellite imagery and air-borne laser altimetry. Furthermore, numerous historic river plans are available which indicate river widths and the simple linear regression might be used to estimate historic bankfull discharges.

6.3 Channel Gradient

Regression models for channel gradient at bankfull (derived from the hydraulic modelling) was more strongly correlated with the valley bottom flatness index (MrVBF) than with the channel gradient derived from the digital elevation model. This most likely reflects the difficult of estimating longitudinal gradients along river channels from digital elevation models (DEM). As might be expected, bankfull slope decreased with both valley bottom flatness and the 1.58 year unregulated flood magnitude. Modelling provides a better estimate of bank full slope than measurement from DEMs that have poor accuracy in elevation.

Regression equations for the bankfull channel gradient have correlation coefficients between 0.54 and 0.64. These correlations may seem unexpected low but can be explained by the large uncertainty in estimation of bankfull slope. We estimate that 34% of the variance in bankfull slope (log-transformed) is due to estimation errors. If these estimates are correct, the maximum correlation coefficients we can expect for our regression equations where bankfull slope is the dependent variable are 0.66, the remaining variance being the consequence of slope estimation errors. In this light, the regression equations seem particularly strong with most variance being explained either by the dependent variables or slope estimation error.

6.4 Channel Shape

Meander wavelength was the primary variable explaining cross-sectional shape parameters for the river channels although correlations were generally quite weak. Width to depth ratios generally increased with meander wavelength and ratio of wetted perimeter to surface width at bankfull decreased. The ratio of maximum depth to mean depth indicates the prominence of bars and in-channel benches. We found that this ratio generally increased with the PET/Rainfall ratio which relates to streamflow variability. The results suggest that there is more cross-sectional variability (associated with benches and bars) in rivers with greater flow variability. The ratio decreases with increasing meander wavelength suggesting more variable cross-section in channels with high bank resistance. But the correlation coefficients for all these relations are low. A closer examination of the nature of these relations is needed before firm conclusions can be reached.

No significant relation was found between bankfull width variability and catchment parameters and there was only a weak positive relation between variability in bankfull depth and channel slope. Particularly absent was any relationship with riparian woody cover which could be a consequence of errors due to the GIS technique employed and source (BRS Land Cover) data and this aspect warrants closer investigation using better maps of vegetation extent. Uncertainty in the parameters describing channel variability is large which may in part explain limited success obtaining significant regression relations.

6.5 At-A-Station Hydraulic Geometry

The change point discharge for width and depth reach hydraulic geometry relations increases with flow magnitude, channel gradient and meander wavelength. The most useful relation for predicting the Q_{CP} is the simple regression equation with bankfull width which explains 36% of the variance in the change point discharge. A further 40% is associated with errors in estimating the change point discharge. Stronger correlations are obtained using slope and bankfull discharge but these relations are likely to be strongly influenced by errors in variable estimates and include spurious correlations.

The width exponent parameters (θ_{W2} and θ_{W3}) are not well correlated with any of the independent variables and probably best treated as constants. The average values for these parameters are 0.235 and 0.0112 respectively. The width coefficient a_2 is positively related to the meander wavelength and flow magnitude with the most useful relation obtained using the Group 3 set of independent variables which gives the coefficient as a power function of mean unregulated flow and meander wavelength with a correlation coefficient of 0.45. A substantial portion of the unexplained variance is likely to be a consequence of errors estimating the coefficient.

As with width, the Group 3 independent variables provide the most useful regression models for the depth exponent parameters (θ_{D2} and θ_{D3}). For these two parameters 66% and 75% of the variance is associated with estimation errors. The regression models explain 65% and 50% (for θ_{D2} and θ_{D3} respectively). The mean exponent θ_{D2} is positively related to the catchment slope and θ_{D3} is positively related to meander wavelength and the mean unregulated flow.

References

Andrews, E.D. (1984). Bed-material entrainment and hydraulic geometry of gravel-bed rivers in Colorado. *Geological Society of America Bulletin* 95: 371- 378.

ASCE (1998). River width adjustment. II: Modeling. ASCE Task Committee on hydraulics, bank mechanics, and modelling of river width adjustment, Journal of Hydraulic Engineering. 124: 903-917.

Blench, T. (1951). Regime theory for self-formed sediment-bearing channels. *Proc. Am. Soc. Civil. Engrs.* 77.

Blench, T. (1957). *Regime Behavior of Canals and Rivers*. Butterworth, London

Brierly, G.J. and Hickin, E.J. (1985). The downstream gradation of particle sizes in the Squamish River, British Columbia. *Earth Surface Processes and Landforms* 10: 597 - 606.

Brunner, G.W. (2001). HEC-RAS River Analysis System: Hydraulic Reference Manual, Version 3.0. Davis, California, U.S. Army Corps of Engineers.

Buhman, D.L., Gates, T.K. and Watson, C.C. (2002). Stochastic variability of fluvial hydraulic geometry: Mississippi and red rivers. ASCE Journal of Hydraulic Engineering 128:426-437.

Dingman, S.L. and Scharma, K.P. (1997). Statistical development and validation of discharge equations for natural channels. *Journal of Hydrology* 1991: 13 35.

Eaton, B.C. and Miller, R.G. (2004). Optimal alluvial channel width under a bank stability constraint. *Geomorphology* 62:35-45.

Gallant, J.C. and Dowling, T.I. (2003). A multi-resolution index of valley bottom flatness for mapping depositional areas. *Water Resources Research* 39 (12): 1437.

Graf, W.H. (1971). *Hydraulics of Sediment Transport*. McGraw-Hill, New York.

Henderson, F.M. (1966). *Open Channel Flow.* Macmillan NY.

Hey, R.D. and Thorne, C.R. (1986). Stable channels with mobile gravel beds. *J. Hydraul. Eng.* 112: 671 689.

Hicks, D.M. and Mason, P.D. (1991). Roughness Characteristics of New Zealand Rivers. Wellington, New Zealand, Water Resources Survey, DSIR Marine and Freshwater.

Huang, H.Q. and Nanson, G.C. (1997). Vegetation and channel variation; a case study of four small streams in southeastern Australia. *Geomorphology*, 18, 237-249.

Johnson, P.A. (1996). Uncertainty of hydraulic parameters. ASCE Journal of Hydraulic Engineering 122:112-114.

Jowett, I.J. (1998). Hydraulic geometry of New Zealand Rivers and its use as a preliminary method of habitat assessment. *Regul. Rivers: REs. Mgmt.* 14: 451 4466.

Kennedy, R.G. (1895). The prevention of silting in irrigation canals. *Min. Proc. Inst. Civil Engrs.* CXIX.

Knighton, D. (1984). *Fluvial Forms and Processes.* London, Edward Arnold.

Knighton, L.B. (1975). Variations in at-a-station hydraulic geometry. *American Journal of Science* 275: 186-218.

Lacey (1929). Stable channels in Alluvium. *Min. Proc. Inst. Civil Engrs*. 229.

Lamouroux, N. and Suchon, Y. (2002). Simple predictions of instream habitat model ouputs for habitat guilds in large streams. *Freshwater Biology* 47(8), 1531-1542.

Lamouroux, N. and Capra, H. (2002). Simple predictions of instream habitat model ouputs for target fish populations. *Freshwater Biology* 47(8), 1543-1556.

Lang, S., Ladson, T. and Anderson, B. (2004). A review of empirical equations for estimating roughness and their applications to four streams in Victoria. *Australian Journal of Water Resources* 8(1): 1-14.

Leopold, L.B. and Maddock, T. (1953). The hydraulic geometry of stream channels and some physiographic implications. *U.S. Geol. Survey Prof. Paper 252.*

Leopold, L.B., Wolman, M.G. and Miller, J.P. (1964). *Fluvial processes in Geomorphology*. W.H. Freeman and Company, San Fransisco, California, 522 pp.

Leopold, L.B. (1994). *A view of the River*. Harvard University Press, Cambridge, Massachusetts

Lewis, C.A., Lester, N.P., Bradshaw, A.D., Fitzgibbon, J.E., Fuller, K., Hakanson, L. and Richards, C. (1996). Consideration of scale in habitat conservation and restoration. *Canadian Journal Aquat. Sci* 53(Suppl. 1): 440-445.

Lindley, E.S. (1919). Regime Channels. *Proc. Punjab. Eng. Congr. VII.*

Manly, B.F.J. (1997). Randomization, Bootstrap and Monte Carlo Methods in Biology. London, Chapman and Hall

Pilgrim, D.H. (1987). Australian rainfall and runoff: a guide to flood estimation. The Institute of Engineers, Australia.

Pitlick, J. and Cress, R. (2002). Downstream changes in the channel geometry of a large gravel bed river. *Water Resources Research* 38 (10): 1 11.

Rhoads, B.L. (1992). Statistical models of fluvial systems. *Geomorphology* 5: 433-455.

Richards, K.S. (1982). *Rivers: form and process in alluvial channels.* Methuen, London.

Riggs, H.C. (1976). A simplified slope-area method for estimating flood discharges in natural channels. Pages 285-291 *in* Journal Research U.S. Geological Survey.

Schumm, S.A. (1960). The shape of alluvial channels in relation to sediment type. *US Geol. Surv. Prof. Paper* 325B.

Schumm, S.A. (1977). *The Fluvial System*. Wiley.

Simons, D.B., Richardson, E.V. and Haushild, W.L. (1962). Depth-Discharge relations in alluvial channels. *Proc. Am. Soc. Cicil. Engnrs* 88 (HY5).

Singh, K.P. and McConkey, S. (1989). Hydraulic geometry of streams and stream habitat assessment. *Journal of Water Resources Planning and Management* 115: 583-597.

Stewardson, M.J. (2005). Hydraulic geometry of stream reaches. *Journal of Hydrology* 306: 97-111.

Western, A.W., Finlayson, B.L., McMahon, T.A. and O'Neill, I.C. (1997). A method for characterising longitudinal irregularity in river channels. *Geomorphology*. 21: 39-51.

White, W.R., Bettess, R. and Paris, E. (1982). Analytical approach to river regime. *Journal of the Hydraulics Division, ASCE* 108: 1179-1193.

Wilkinson, S., Henderson, A. and Chen, Y. (2004). SedNet: A CSIRO Land and Water client report for the CRC for Catchment Hydrology. Version 1. *CSIRO Land and Water, Canberra.* 76p.

Wilkinson, S.N., Young, W.J. and DeRose, R.C. (in press). Regionalising Mean Annual Flow and Daily Flow Variability for Basin-scale Sediment and Nutrient Modelling. *Hydrological Processes.*

Appendix I: Methods Used in Uncertainty Analysis

The uncertainty inherent in hydraulic modelling comes from several sources – errors in the channel survey, appropriateness of the chosen model and uncertainty in the model parameters to name but a few. In this study an attempt has been made to quantify the effect of parameter uncertainty on the hydraulic model results, in particular the error resulting from uncertainty in Manning's *n* and the downstream boundary condition.

The sensitivity of hydraulic model outputs to uncertainties in their inputs has been examined previously, but in most of the studies, an error model has been assumed rather than constructed from data. Johnson (1996) presents a review of these studies from the perspective of reliability analysis. Reliability analysis depends on having some idea of how uncertain the parameters underlying the design model are. As Johnson (1996) states, in uncertainty analysis "the analyst typically assumes some values of parameter uncertainties for the purposes of illustration, but without accurate information on uncertainty, the uncertainty analysis may not be meaningful." The challenge is therefore to develop accurate distributions for the input parameters.

In most reliability studies, error in Manning's *n* has been assumed to be normally distributed and a value of the coefficient of variation has been more or less arbitrarily adopted (Johnson 1996). An exception is Buhman (1986), who examined error in estimating Manning's *n* by visual assessments. A group of 77 engineers were asked to estimate Manning's *n* for 10 stream reaches. That study found that the estimates were best described with a log normal distribution with a CV that increased with increasing mean estimates of Manning's *n* from 20% to 35% for n between 0.02 and 0.06. No assessment of the true value of Manning's *n* was made, so systematic errors in the visual estimation of Manning's *n* could not be assessed.

Empirical equations offer a consistent, unbiased, repeatable method of choosing Manning's *n* at each site. The Dingman and Sharma (1997) empirical equation carried the added benefit of having a documented error distribution. Dingman and Sharma (1997) used the data compiled by Hicks and Mason (1991) to derive a version of Manning's equation that does not include a roughness parameter. By equating this relationship to Manning's equation, an equation predicting Manning's *n* can be derived:

$$n = 0.217A^{1.173}R^{0.267}S^{0.156}$$

Dingman and Sharma (1997) publish the cumulative distribution of errors for their model. Log errors of the Dingman and Sharma (1997) model were approximately normally distributed with some deviations at the tails. Rather than assuming a normal distribution for the error model and calculating its moments from the observed data, the observed distribution of errors was used directly. This error model has the advantage of being free of systematic error and completely objective.

The effects of error at the downstream boundary condition has received less investigation than error in Manning's *n*, though there is little to suggest it is less significant, particularly for shorter or low gradient reaches. The slope used is often estimated using the average channel slope obtained from topographic maps.

Johnson (1996) reports two studies where sensitivity to the slope has been investigated, but neither of these studies details how the initial slope error distribution was determined. Johnson (1996) reports a value for the coefficient of variation based on an experiment where a group of students was asked to determine channel slope from a contour map. While the measurement error found in that study is significant, it can be reduced by the use of accurate maps and computer algorithms to calculate slope. Two other sources of error remain.

A systematic error will occur in low gradient reaches where the map contours are too widely spaced to provide an accurate assessment of the channel slope over a short distance. The naturally concave profile of

many rivers will lead to an underestimation of reach slope where a reach falls just below a contour and an over-estimation where it falls just above. Other data, such as flood-height measurements provide a more accurate basis for estimating channel slope at these points.

Finally, and perhaps most importantly, the actual slope at the downstream boundary is not the same as the mean channel slope. There is a distribution of slopes in a reach around the mean channel slope, and the downstream boundary could take any value from this distribution.

To asses this error, an error model for slope at the downstream boundary was developed based on the distribution of slopes around the mean channel slope in the 114 sites used in this study (a total of 1099 cross-sections, excluding the downstream cross-sections themselves).

The best estimate of slope at the downstream boundary was calculated using 1:25000 scale digital maps and estimates from flood height measurements. Hydraulic models were run at approximately bankfull level with the best estimate available for Manning's *n* and slope. A slope error parameter S_{err} was then calculated as:

$$S_{err} = \log_{10}\left[\frac{S_{xs}}{S_{Best}}\right]$$

where S_{Best} is the best estimate of the slope and S_{xs} is the slope at a cross section. The error model was refined using the assumption that experienced surveyors are unlikely to survey a pool as the downstream cross section. They are more likely to choose a hydraulic control point, such as a riffle. These points can be identified in a reach (to some degree) by bed topography. Three techniques were used to identify pools:

Criterion 1. A pool is any point with a bed slope downstream of it flatter than the best estimate of water surface slope.

Criterion 2. A pool is any point with a bed slope downstream of it flatter than the reach bed slope (slope of regression line through the channel thalweg).

Criterion 3. A pool is any point that lies below the line of best fit between the thalweg points.

These three procedures each identified about half the cross sections as being pools. Using the remaining cross sections, the distribution of S_{err} was again calculated. The results are given in the following Table.

		All	Pools Removed		
			Criterion 1	Criterion 2	Criterion 3
Number of XS		1099	536	527	571
Q =	**S_{err}**				
1/10 Bankfull	mean	-0.17	0.33	0.30	0.28
	st.dev	1.06	0.96	1.00	0.89
Bankfull	mean	-0.07	0.09	0.06	0.06
	st.dev	0.60	0.56	0.58	0.56

These results suggest that the errors in the downstream boundary condition could be modeled by a log-normal distribution with a mean of 0.07 and a standard deviation of 0.57. That is:

$$\hat{S} = S_{Best} \times 10^{N}$$

Where $\hat{S}$ is an estimate of the slope, N is a random normal deviate with mean of 0.07 and a standard deviation of 0.57. This of course implies that there is a systematic error in the estimation of downstream boundary condition using the procedures described above. Slopes from topographic maps tend to underestimate slope at riffles by about 15%.

The derived error distributions for Manning's n and downstream boundary condition were used to estimate the error in the hydraulic model outputs using a Monte-Carlo approach (Manly, 1997). This approach simply involves repeatedly running the hydraulic model using a random sample of input parameters from their (known) distribution. The distribution of the output parameters can then be from the sample output. In each Monte-Carlo run, 500 random parameter samples were used giving 500 replicate model runs. Hydraulic Geometry and Bankfull characteristics were determined for each replicate model runs. The distributions of the resulting parameters represent the uncertainty in the parameter estimates emanating from uncertainty in model input parameters.

Appendix II: Hydrological Regionalisation

Since the surveys locations rarely coincide with gauging stations then interpolation of river flows to these locations is necessary. To do this, the hydrological regionalisation method described by Wilkinson *et al.,* (in press) was applied to 7 hydrographic regions that were contiguous and broadly similar in terms of geography and rainfall. These were: the Goulburn-Broken (GB), Ovens-Kiewa-Upper Murray (OKM), East Gippsland (GE), South Gippsland (GS), Melbourne catchments (MLB), South Coast catchments (to Glenelg R)(SC), and Wimmera-Loddon-Campaspe (WLC) catchments.

A link-node and associated watershed representation of the river network was built from the 9" (≈250 m) digital elevation model (DEM) of Australia (AUSLIG 1996) using ArcInfo™ Macro Language (AML) scripts similar to those employed by Prosser *et al.,* (2001) in construction of their river sediment network model (SedNet). The DEM network was ordered (modified Shreve) and a network accumulation algorithm was used to calculate the upstream contributing area, average precipitation (P) and potential evaporation (E_0), from the grid (cell) means of the watershed areas associated with each river link. The point location of gauging stations were spatially joined to the DEM river network, and the mean annual rainfall runoff coefficient (R_c) calculated at each station, was non-linearly regressed against the ratio of E_0/P to enable interpolation of R_c and hence Q_a ($=R_c.A_c.P$) throughout the river network. The technique produced relative RMS errors for predicted versus observed Q_a of between 32 and 41 % for the 7 regions. These encompass the majority (75 to 90 %) of observations and only a small percentage (< 5%) had errors > 80 % of the observed value.

The ARI flows $Q_{0.5}$ to Q_{10} were first correlated with Q_a and σ_d at gauging stations (Table 1). σ_d is an index of daily flow variability ($\sigma_d = \sum(Q_d / \bar{Q}_d)^{1.4}$) which can be correlated with mean annual rainfall ($\sigma_d = cP^d + 1$, c and d are constants), allowing interpolation between stations. The resultant functional relationships between ARI flows and Q_a and σ_d (Table 1) allowed for interpolation of these flows throughout the river network. Correlation was generally high in LLS regressions (R^2 > 80%), but because of added uncertainty in predicted Q_a and σ_d at survey locations, relative RMS-errors of 41 67 % for predicted versus observed $Q_{0.5}$ - Q_{10} were generally greater than for Qa alone. Comparison of neighboring gauging stations showed there was systematic spatial variation in error across basins, allowing for localised corrections to be made at each survey location based on the average percentage error with the three closest gauging stations.

Table 7. Regional Equations used to Interpolate ARI Flows.

Region	ARI (years)	$ARI = aQ^b.10^{(\sigma_d f)}$			
		a	b	f	R^2
GB	0.5	0.0535	0.818	0.271	0.93
	1	0.0750	0.801	0.326	0.92
	1.5	0.041	0.872	0.347	0.94
	2	0.0507	0.863	0.346	0.94
	5	0.0912	0.838	0.349	0.93
	10	0.128	0.825	0.353	0.91
OKM	0.5	0.00247	0.963	0.685	0.98
	1	0.00320	0.958	0.728	0.97
	1.5	0.00427	0.943	0.755	0.98
	2	0.00478	0.937	0.768	0.97
	5	0.00621	0.920	0.834	0.96
	10	0.00698	0.909	0.892	0.95
GE	0.5	0.0202	0.936	0.162	0.98
	1	0.0223	0.926	0.329	0.98
	1.5	0.0244	0.924	0.401	0.98
	2	0.0264	0.922	0.419	0.97
	5	0.0369	0.910	0.460	0.96
	10	0.0480	0.901	0.477	0.96
GS	0.5	0.0213	0.940	0.151	0.88
	1	0.0228	0.910	0.329	0.91
	1.5	0.0363	0.870	0.384	0.89
	2	0.0406	0.867	0.396	0.89
	5	0.0628	0.848	0.434	0.90
	10	0.0877	0.831	0.461	0.89
MLB	0.5	0.00471	1.149	0.087	0.97
	1	0.00542	1.130	0.193	0.98
	1.5	0.00537	1.131	0.257	0.98
	2	0.00580	1.128	0.273	0.98
	5	0.00885	1.106	0.311	0.98
	10	0.0130	1.086	0.328	0.98
SC	0.5	0.0162	0.867	0.417	0.96
	1	0.0163	0.874	0.504	0.97
	1.5	0.0179	0.886	0.510	0.96
	2	0.0197	0.891	0.502	0.96
	5	0.0261	0.903	0.480	0.95
	10	0.0311	0.912	0.467	0.93
WLC	0.5	0.00973	0.961	0.329	0.91
	1	0.0131	0.952	0.391	0.96
	1.5	0.0124	0.965	0.434	0.96
	2	0.0142	0.960	0.436	0.97
	5	0.0248	0.936	0434	0.97
	10	0.0382	0.916	0.427	0.97

Region	$\sigma_d = cP^d + 1$		
	c	d	R^2
GB	1.16×10^6	-2.10	0.79
OKM	1.22×10^4	-1.43	0.45
GE	6.24×10^3	-1.32	0.12
GS	4.98×10^{10}	-3.58	0.59
MLB	2.47×10^9	-3.21	0.46
SC	2.31×10^3	-1.17	0.61
WLC	2.91×10^3	-1.21	0.44

Appendix III: Plots of Modelled and Observed Channel Metrics

The following 106 plots correspond to the 106 regression equations presented in Chapter 5 and labeled using the same equation numbering. The X-axis gives the value of channel metrics derived from channel surveys and hydraulic modelling. The Y-Axis gives the value of the same metric estimated by the regression equation. Plots show un-transformed parameter values (although log-axis have been used for bankfull discharge and change point discharge) using S.I. units.

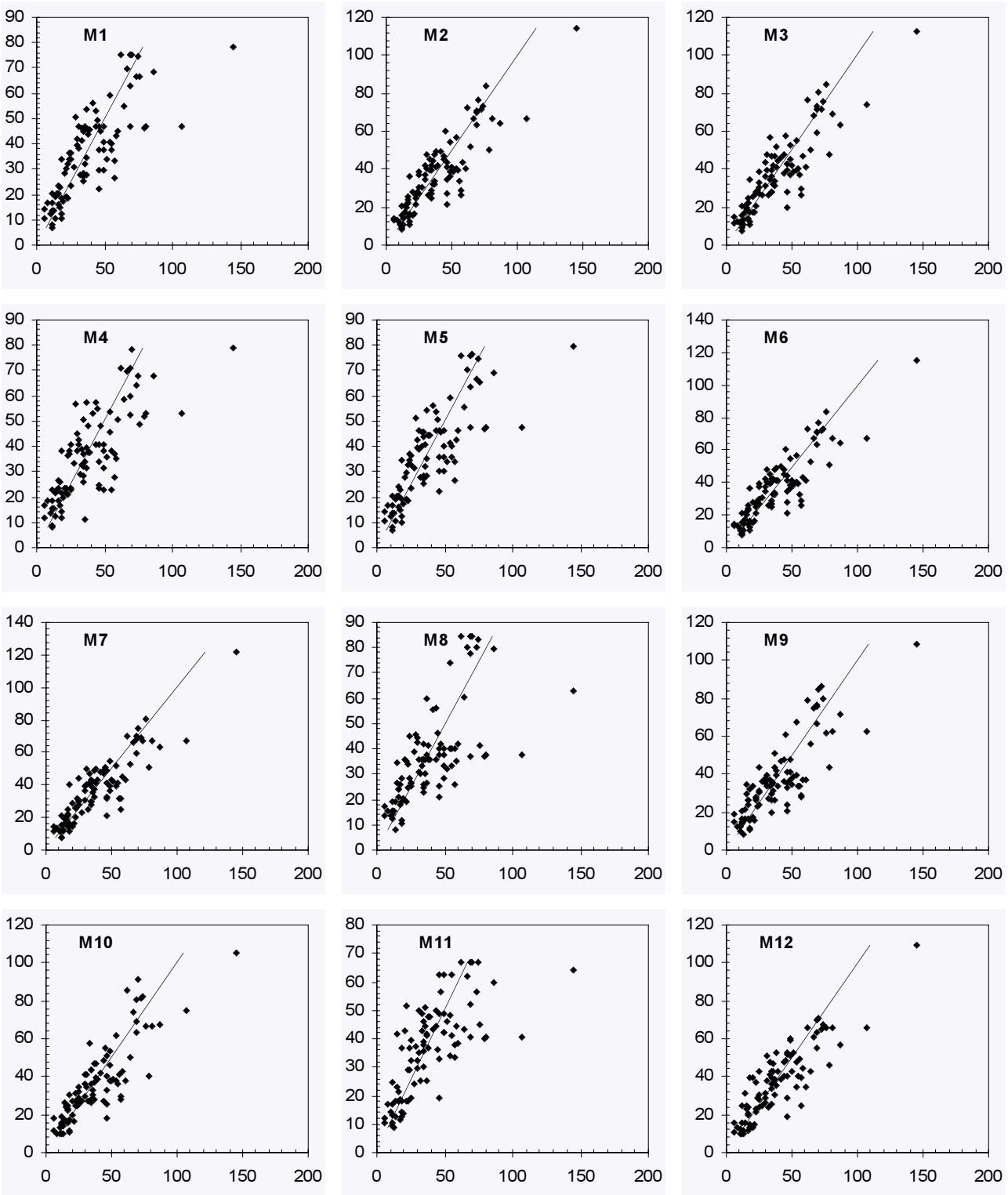
M1
M2
M3
M4
M5
M6
M7
M8
M9
M10
M11
M12

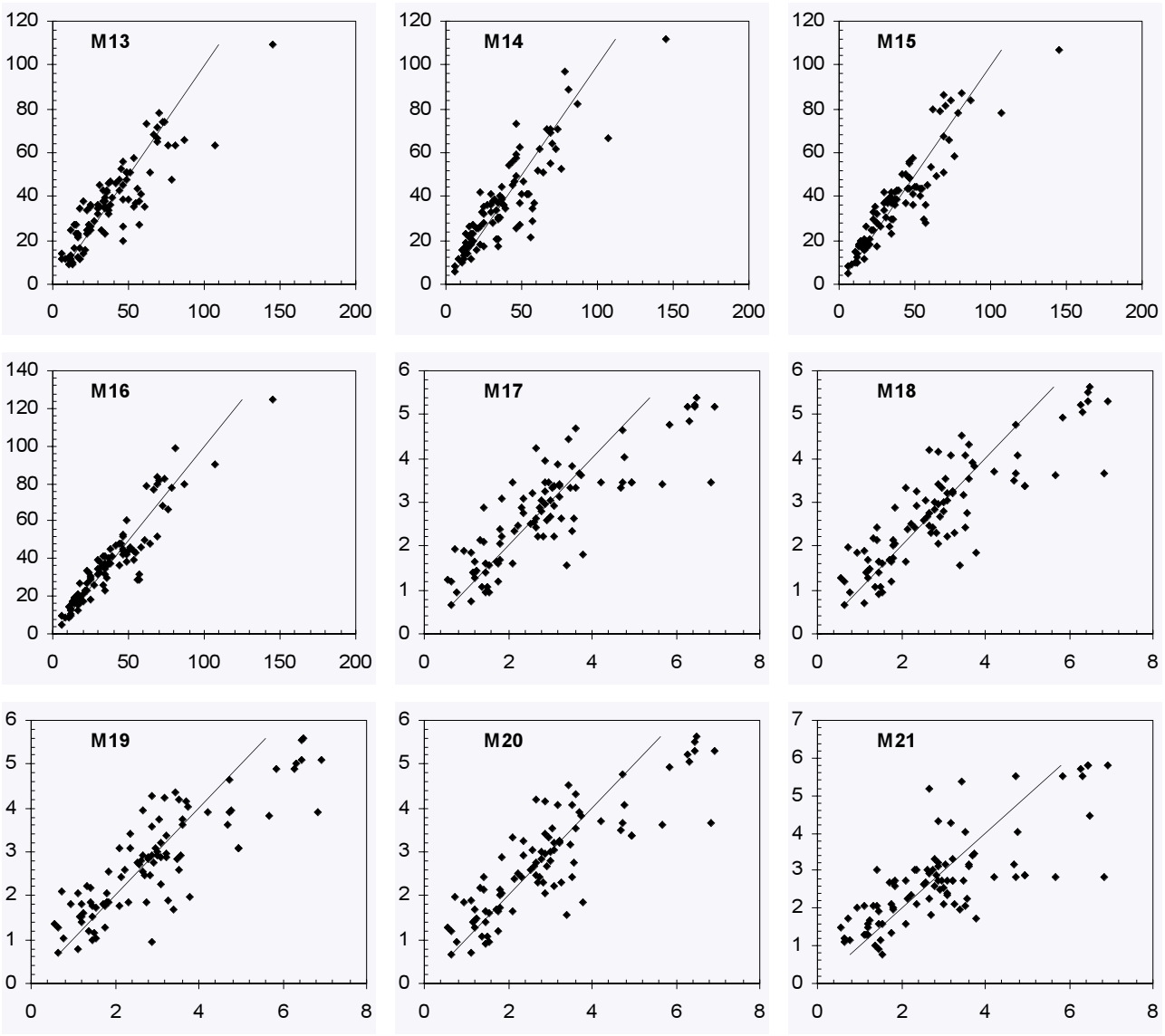
M13
M14
M15
M16
M17
M18
M19
M20
M21

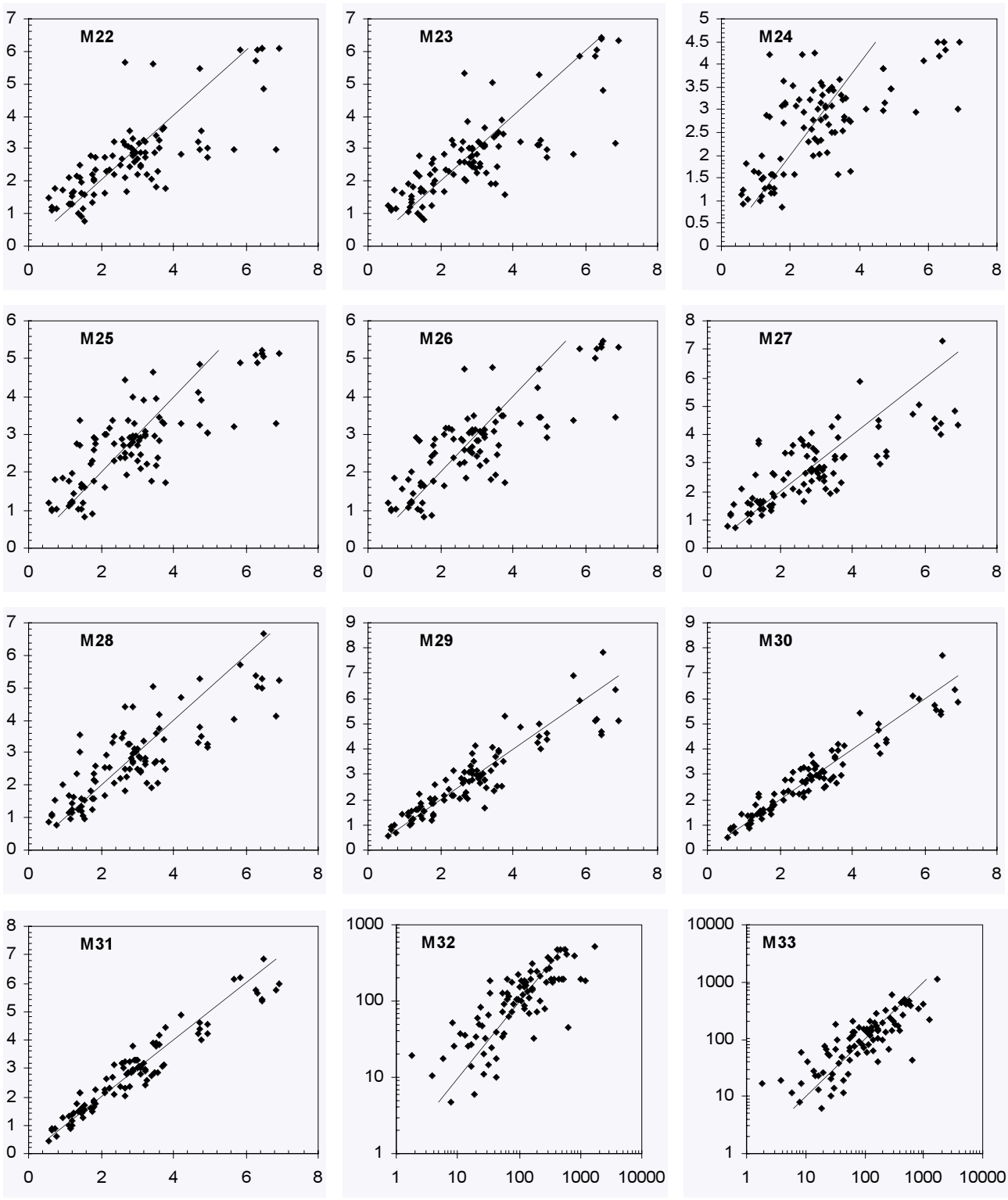
M22
M23
M24
M25
M26
M27
M28
M29
M30
M31
M32
M33

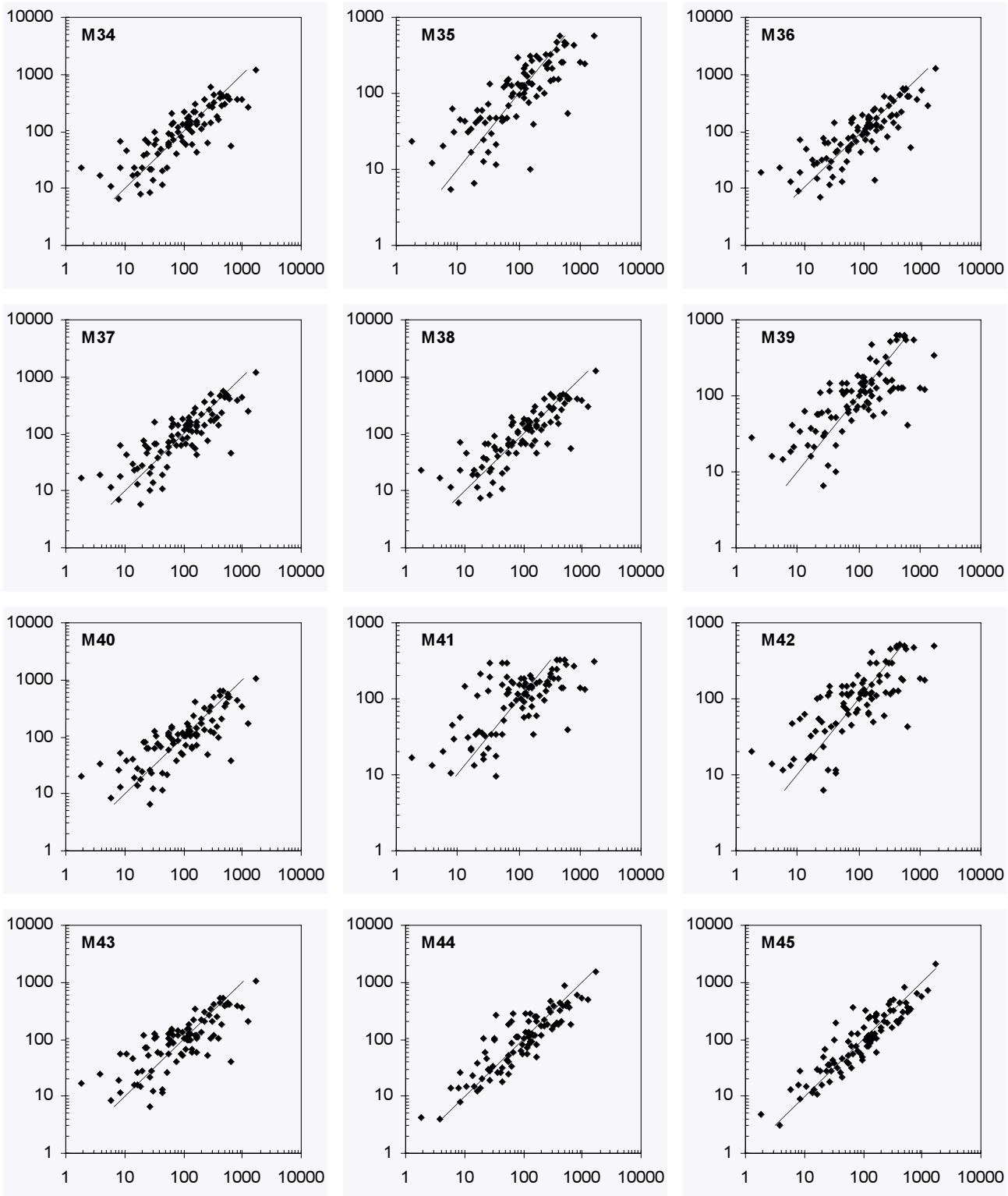
M34
M35
M36
M37
M38
M39
M40
M41
M42
M43
M44
M45

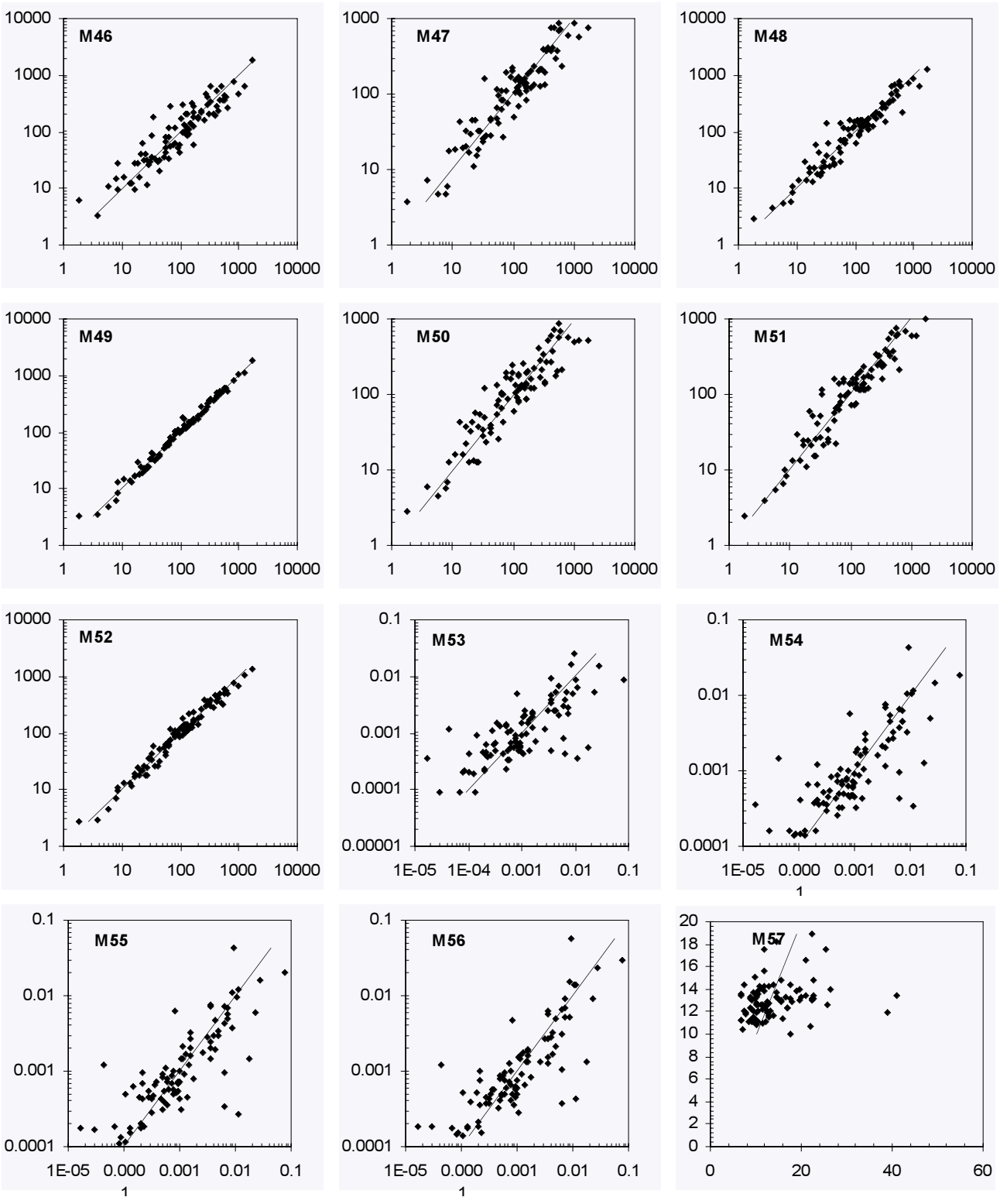
M46
M47
M48
M49
M50
M51
M52
M53
M54
M55
M56
M57

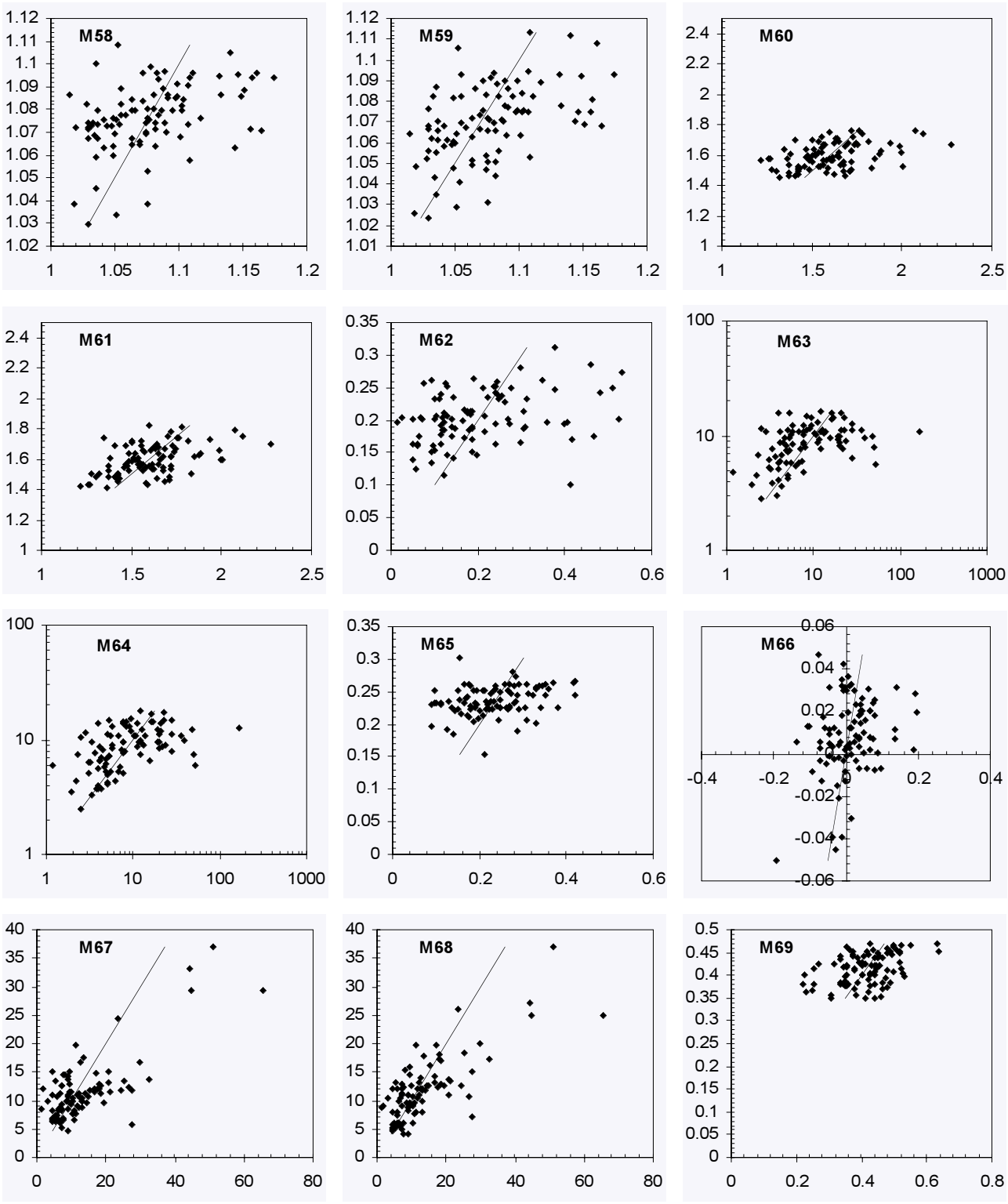
M58
M59
M60
M61
M62
M63
M64
M65
M66
M67
M68
M69

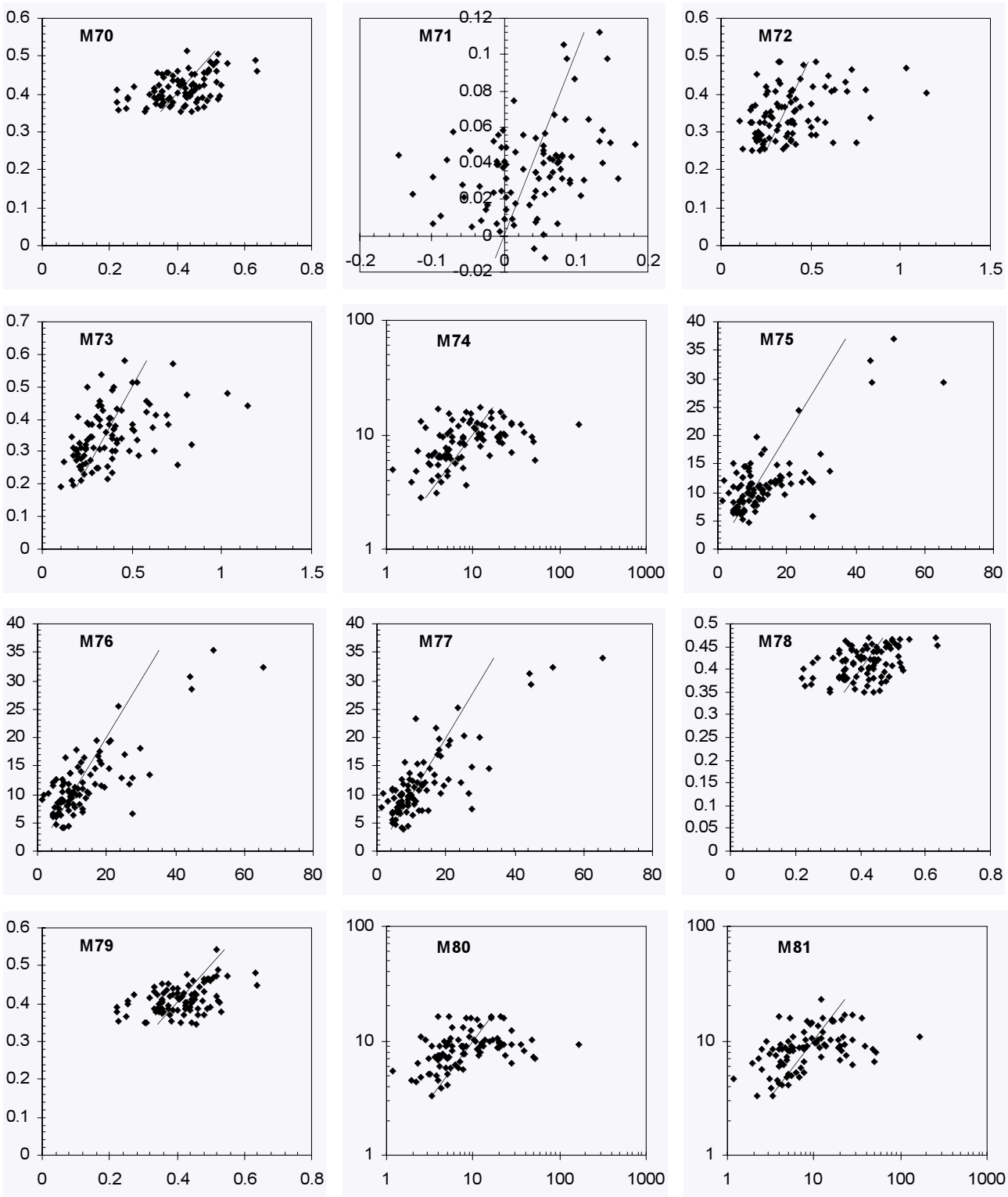
M70
M71
M72
M73
M74
M75
M76
M77
M78
M79
M80
M81

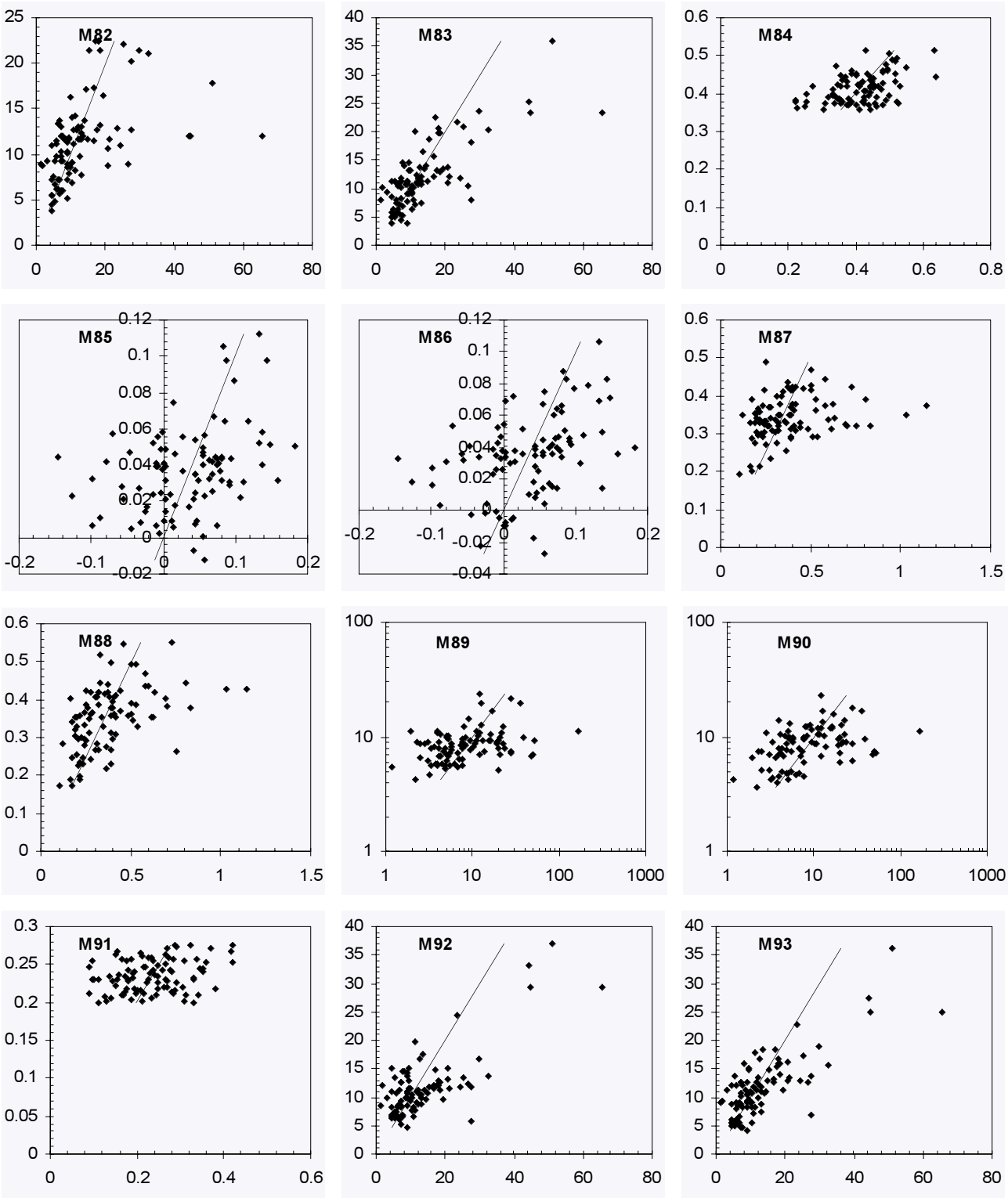
M82
M83
M84
M85
M86
M87
M88
M89
M90
M91
M92
M93

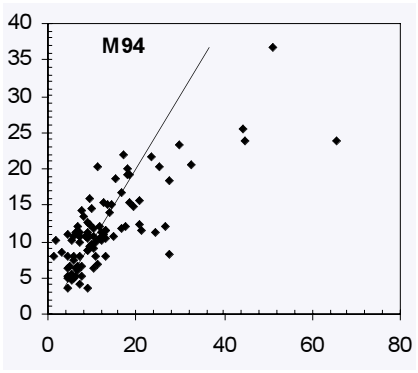
M94
0 5 10 15 20 25 30 35 40
0 20 40 60 80

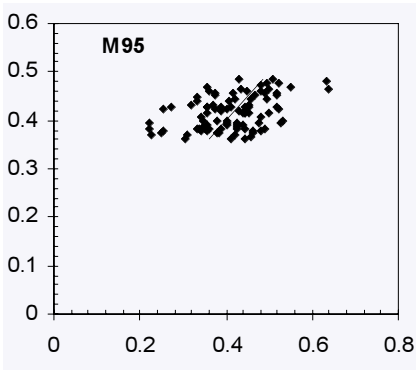
M95
0 0.1 0.2 0.3 0.4 0.5 0.6
0 0.2 0.4 0.6 0.8

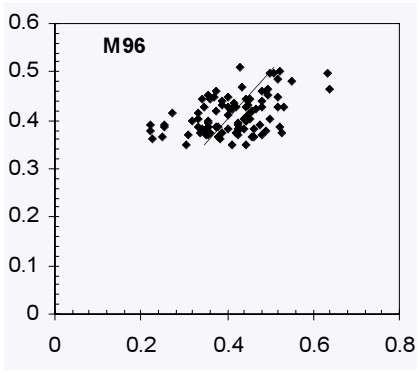
M96
0 0.1 0.2 0.3 0.4 0.5 0.6
0 0.2 0.4 0.6 0.8

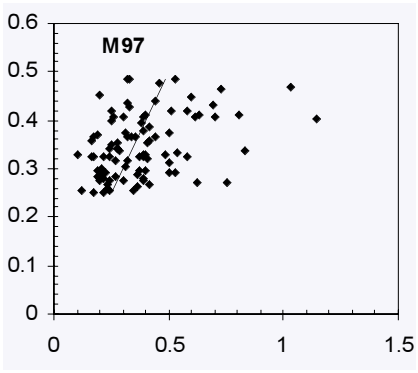
M97
0 0.1 0.2 0.3 0.4 0.5 0.6
0 0.5 1 1.5

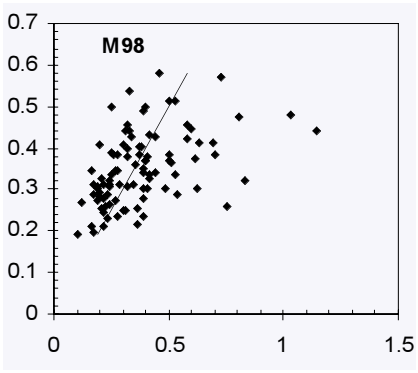
M98
0 0.1 0.2 0.3 0.4 0.5 0.6 0.7
0 0.5 1 1.5

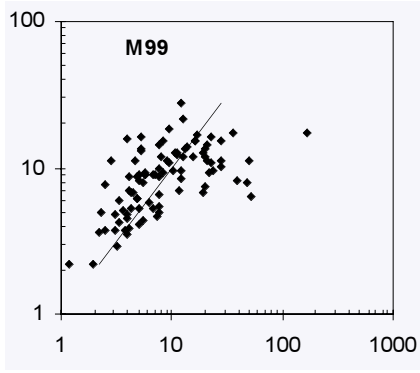
M99
1 10 100
1 10 100 1000

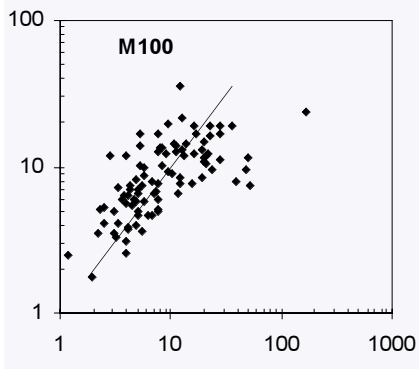
M100
1 10 100
1 10 100 1000

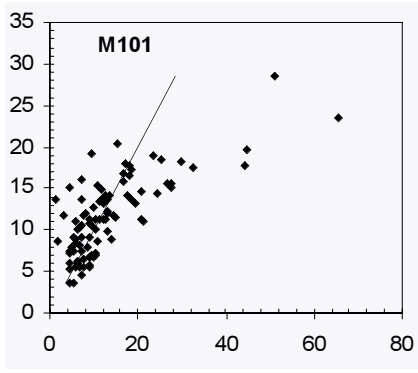
M101
0 5 10 15 20 25 30 35
0 20 40 60 80

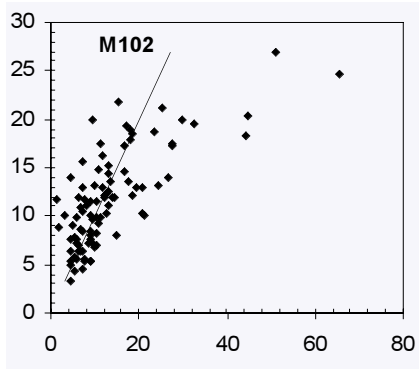
M102
0 5 10 15 20 25 30
0 20 40 60 80

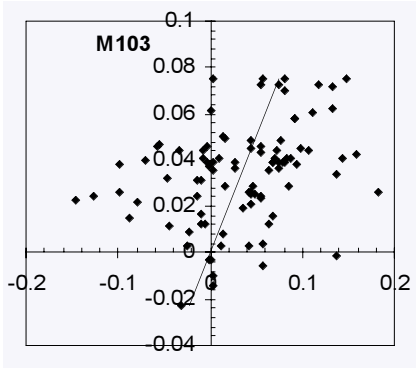
M103
-0.04 -0.02 0 0.02 0.04 0.06 0.08 0.1
-0.2 -0.1 0 0.1 0.2

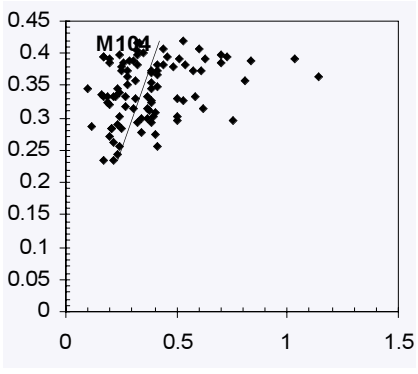
M104
0 0.05 0.1 0.15 0.2 0.25 0.3 0.35 0.4 0.45
0 0.5 1 1.5

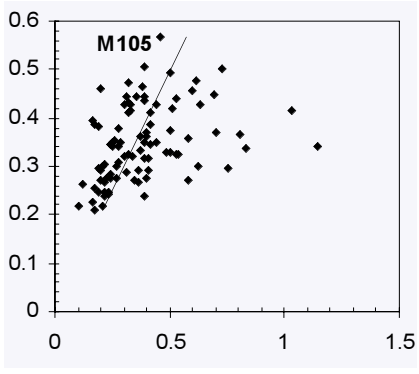
M105
0 0.1 0.2 0.3 0.4 0.5 0.6
0 0.5 1 1.5

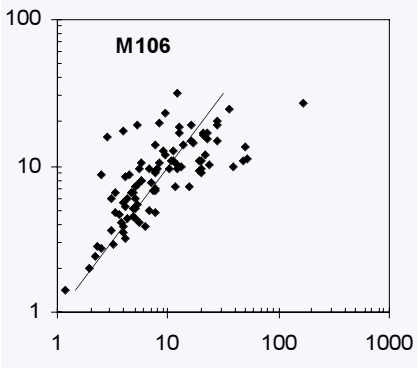
M106
100
10
1
1
10
100
1000

CENTRE OFFICE

CRC for Catchment Hydrology
Department of Civil Engineering
Building 60
Monash University
Victoria 3800
Australia

Tel +61 3 9905 2704
Fax +61 3 9905 5033
email crcch@eng.monash.edu.au
www.catchment.crc.org.au

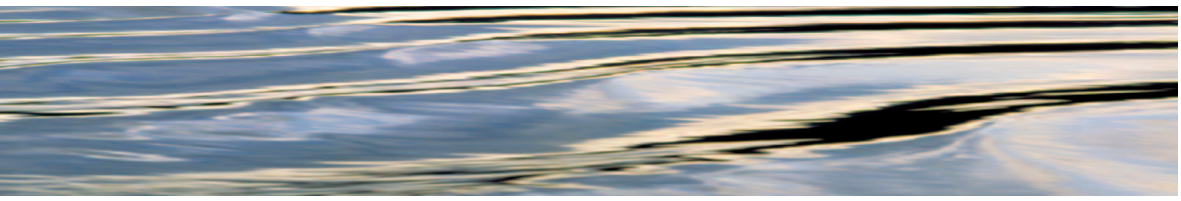

The Cooperative Research Centre for Catchment Hydrology is a cooperative venture formed under the Australian Government's CRC Programme between:

- Brisbane City Council
- Bureau of Meteorology
- CSIRO Land and Water
- Department of Infrastructure, Planning and Natural Resources, NSW
- Department of Sustainability and Environment, Vic
- Goulburn-Murray Water
- Grampians Wimmera Mallee Water
- Griffith University
- Melbourne Water
- Monash University
- Murray-Darling Basin Commission
- Natural Resources and Mines, Qld
- Southern Rural Water
- The University of Melbourne

ASSOCIATE:

- Water Corporation of Western Australia

RESEARCH AFFILIATES:

- Australian National University
- National Institute of Water and Atmospheric Research, New Zealand
- Sustainable Water Resources Research Center, Republic of Korea
- University of New South Wales

INDUSTRY AFFILIATES:

- Earth Tech
- Ecological Engineering
- Sinclair Knight Merz
- WBM

CRC AUSTRALIA

Established and supported under the Australian Government's Cooperative Research Centre Program

COOPERATIVE RESEARCH CENTRE FOR
CATCHMENT HYDROLOGY